GEOLOGY AND MECHANICS OF THE BLACKHAWK LANDSLIDE, LUCERNE VALLEY, CALIFORNIA

Thesis by

Ronald Lee Shreve

In Partial Fulfillment of the Requirements

For the Degree of

Doctor of Philosophy

California Institute of Technology

Pasadena, California

1959

ACKNOWLEDGMENTS

It is a pleasure to thank R. P. Sharp, who first showed me the Blackhawk rockslide and who supervised this research, for his constant support and invariably helpful suggestions, and to thank W. B. Kamb and W. D. Rannie for their constructive criticisms of the air-lubrication theory.

This work was entirely supported by grants made by the California Institute of Technology and the National Science Foundation.

ABSTRACT

Blackhawk Mountain, a resistant mass of marble thrust northward over uncemented sandstone and weathered gneiss, rises above southeastern Lucerne Valley at the eastern end of the rugged 4000-foot escarpment that separates the San Bernardino Mountains on the south from the Mojave Desert on the north. Spread out on the alluvial apron at the foot of the mountain is the Blackhawk rockslide, a lobe of nearly monolithologic marble breccia 30 to 100 feet thick, 2 miles wide, and nearly 5 miles long. At least two earlier similar but smaller rockslides have occurred in the area.

The rocks of the area comprise late Tertiary and Quaternary fanglomerates and breccias derived mainly from the gneiss, quartzite, Carboniferous marble, and Cretaceous quartz-monzonite of the San Bernardino Mountains. Uplift of Blackhawk Mountain occurred in two stages after deposition of the older fanglomerates and breccias: the first by over-thrusting from the south, and the second by monoclinal folding along a northwest-trending axis.

Geological evidence in the area shows that the Blackhawk rockslide traversed the gently inclined alluvial slope as a nearly nondeforming sheet of breccia moving more than 50 miles per hour. The hypothesis that compressed air, rather than water or mud, constituted the lubricating layer on which the breccia sheet slid qualitatively explains all of the principal physical features of the slide lobe. Theoretical analysis of the flow in the lubricating air layer indicates the quantitative feasibility of the air-lubrication hypothesis for the Blackhawk slide.

TABLE OF CONTENTS

INTRODUCTION

Lucerne Valley in southern California lies at the foot of the rugged escarpment which drops 4000 feet from the upland valleys and rounded hills of the San Bernardino Mountains on the south to the broad alluvial basins and low peaks of the Mojave Desert on the north. Near the eastern end of this escarpment stands Blackhawk Mountain. Its summit is a resistant mass of marble thrust northward over uncemented sandstone and weathered gneiss. Hence, as a result of undercutting by erosion its north slope is extremely precipitous; in little more than a mile it drops 3000 feet to the mouth of Blackhawk Canyon. Spread out below this very steep slope is a great landslide lobe of nearly monolithologic marble breccia two miles wide and 30 to 100 feet thick which extends five miles from the mouth of Blackhawk Canyon down the gently sloping alluvial apron nearly to the bottom of Lucerne Valley (fig. 1). This is the Blackhawk breccia.

The Blackhawk breccia is notable not only because of the large volume of rock involved but also because of the great horizontal distance travelled from the obvious source on Blackhawk Mountain. Moreover, in travelling this distance it was neither internally lubricated nor slow-moving, like a mudflow, but was a nearly nondeforming sheet of crushed rock which rushed down the gentle alluvial slope at a speed of more than 100 miles per hour.

This paper presents the geological and mechanical evidence from which this conclusion follows, and it proposes an air-lubrication mechanism which explains not only the high speed and undeforming nature of the sliding sheet but also the unusual compositional structure and topo-

FIGURE 1

THE BLACKHAWK AREA

Oblique air photo of the Blackhawk area viewed from the north. Maximum width of the Blackhawk breccia lobe is two miles. Height of its near edge is about 50 feet. (Photo by R. C. Frampton and J. S. Shelton, Claremont, California, 19 September 1948.)

graphic configuration of the resulting lobe of breccia. In addition, this paper shows that the Blackhawk breccia represents the latest of several great landslides which originated on Blackhawk Mountain, and it delineates the structural and stratigraphic developments which led to them.

GEOLOGY OF THE BLACKHAWK AREA

Introduction

The area mapped for this report, herein termed the Blackhawk area, is rectangular, covering about 30 square miles and enclosing Blackhawk Mountain, Terrace Springs, the mouth of Arrastre Canyon, and the alluvial slope for several miles to the north of them in southeastern Lucerne Valley. Elevations in the area range from 3100 feet at the north edge of the Blackhawk breccia lobe through 4500 feet at the head of the alluvial slope to 6800 feet at the summit of Blackhawk Mountain. Creosote bushes, Joshua trees and cholla cactus, and pinyon pines, respectively, comprise the characteristic vegetation at each of these elevations. Gold and silver mines on Blackhawk Mountain have been worked intermittently since 1870 (DeGroot, 1890, p. 523).

The area is geologically divisible into three parts which had different but closely related histories following uplift of the San Bernardino Mountains; these are (a) the gently inclined alluvial slope where deposition of the younger rocks progressed practically without interruption, (b) the steep, thrust-faulted escarpment where deposition and erosion alternated in response to tectonic events, and (c) the dissected mountain highland where erosion of the older rocks proceeded nearly continuously. The stratigraphy and structure of the escarpment, which are described in this section, record in detail the thrust-faulting, folding, fan building, and erosion leading to the landsliding which produced the breccias of the Blackhawk area.

Location and accessibility- The Blackhawk area lies along the central third of the eastern edge of the Lucerne Valley, California, quadrangle of the U. S. Geological Survey approximately 85 miles east of metropolitan Los Angeles. It can easily be reached by automobile via State Highway 18 northeast from San Bernardino through Big Bear Lake, or by the same State Highway southeast from Victorville (fig. 2). A paved County Road leads directly east from the town of Lucerne Valley 10 miles to the north edge of the Blackhawk breccia lobe. A number of unimproved prospectors' roads criss-cross the alluvial slope and lead up onto Blackhawk Mountain.

Previous investigations in the region- In 1922 F. E. Vaughan published a geologic map and report on the old San Gorgonio quadrangle (1:125000), which included the Blackhawk area. Because he was making a reconnaissance map of the region, Vaughan did not differentiate the Blackhawk breccia but simply included it in his Heights fanglomerate.

In 1928 A. O. Woodford and T. F. Harriss published a geologic map of Blackhawk Canyon and with it a brief report covering a much larger area which is practically the same as that described in this paper. They recognized the landslide origin of the breccia and suggested that it was a debris outrush like the slide of 1881 at Elm, Switzerland (Heim, 1882).

In 1953 R. B. Guillou published a map and report on the Johnston Grade area, which adjoins the Blackhawk area on the southwest; and in 1954 J. F. Richmond mapped the region from Big Bear Lake north to the desert, a few miles farther southwest of the Blackhawk area.

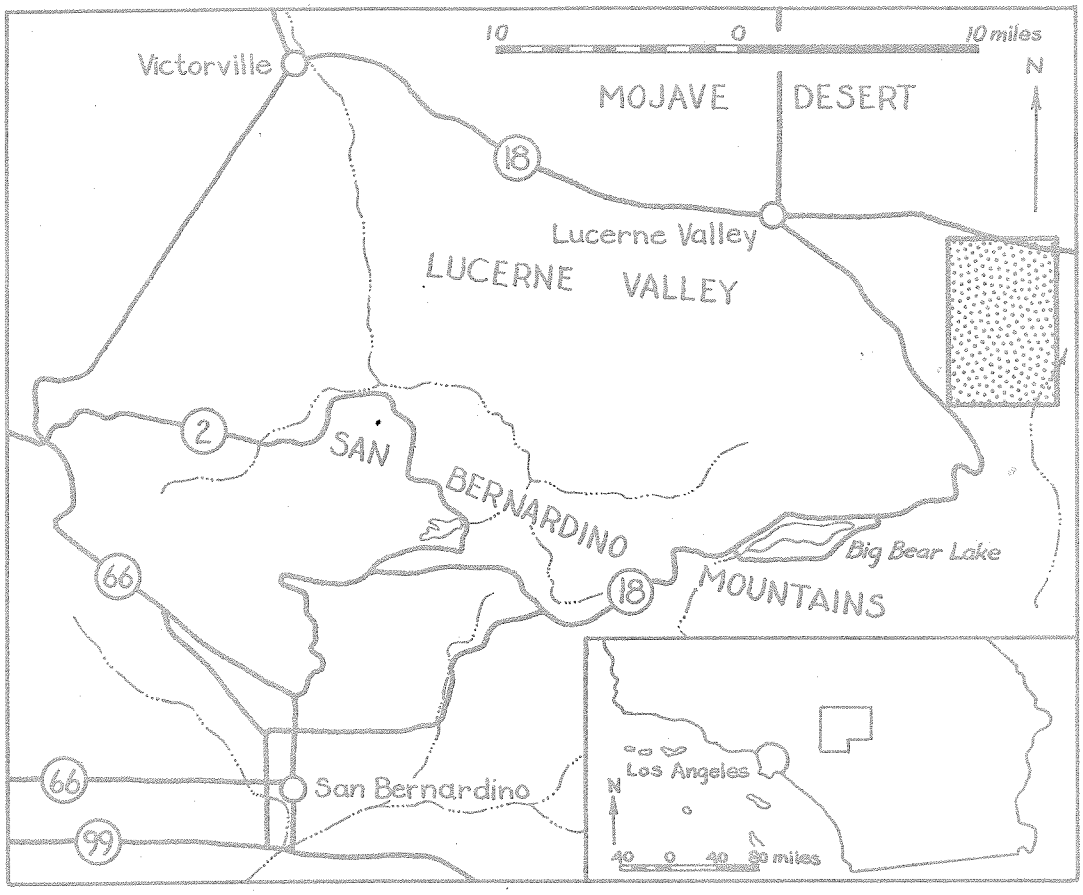

FIGURE 2

INDEX MAP

Location of the Blackhawk area. Geology of the shaded area is shown on Plate 1. Inset shows location of index map relative to Los Angeles.

Present investigation- In 1957 the writer spent about five weeks in the field studying the Blackhawk breccia and making a geologic map of the area (plate 1). Because the objective of this investigation was to find evidence bearing on the origin of the breccia, and especially on its mode of transit down the gently inclined alluvial slope, only those aspects of the geology of the older rocks which are pertinent to the problem of the breccia were studied in detail.

Older rocks

The older rocks in the northern part of the San Bernardino Mountains comprise gneiss, quartzite, and marble which have undergone in succession low-grade regional metamorphism, widespread plutonic intrusion, and extensive large-scale faulting. As a result the stratigraphic sequence of these rocks is not yet satisfactorily determined; neither Guillou (1953) nor Richmond (1954) was able to find conclusive contact relations, though each was able to suggest the probable succession of these rocks. In the Blackhawk area, only the gneiss and the marble, both intruded by quartz-monzonite, are exposed (table 1); and, as elsewhere, they are without exception in fault contact, so that their relative stratigraphic positions are indeterminable.

Undifferentiated gneiss (g)- The Blackhawk area is widely underlain by biotite gneiss intruded by quartz-monzonite. In general, because of their intimate intermingling, these rocks were mapped together as undifferentiated gneiss despite the disparity between them in age and origin. The gneiss exposed in the vicinity of Old Woman Peak and in the foothills east of Arrastre Canyon is typical of this unit. It generally forms steep, rocky, brown hills with somewhat rounded summits.

This unit consists principally of a moderately hard, dark-brown to black, medium- to coarse-grained, prominently foliated, quartz-orthoclase(?)-biotite gneiss in which biotite-rich and biotite-poor foliae alternate at 5 to 10 mm intervals. The foliation of this rock generally is gently undulatory and dips southward, though it is violently contorted locally.

TABLE 1

STRATIGRAPHIC SUMMARY FOR THE BLACKHAWK AREA

Younger rocks	
Fan gravels and minor landslides	Recent
*Cushenbury Springs formation	Pleistocene(?)
*Old Woman sandstone	Pliocene(?)
Older rocks	
Cactus granite	Jurassic/Cretaceous(?)
Furnace limestone	Carboniferous
undifferentiated gneiss and quartz-monzonite	

*New formation defined in this paper.

In the foothills on both sides of the mouth of Arrastre Canyon are extensive outcrops of a hard, light- to reddish-gray, medium- to coarse-grained, prominently foliated and lineated, biotite-quartz-orthoclase(?) gneiss which frequently contains pink quartz-orthoclase augen up to 1 cm in diameter. The foliation transects the contacts between this gray gneiss and the more extensive brown gneiss.

About 2500 feet east of the mouth of Arrastre Canyon irregular lenses of light-gray to black, brown-weathering, fine-grained, crystalline, dolomitic marble up to 50 feet thick are interbedded with the biotite gneiss. This marble is composed of alternating more- and less-dolomitic layers 2 to 3 mm thick that are parallel to the foliation of the proximal gneiss. Also in this area are thin discontinuous lenses of extremely hard, greenish-white, unlaminated and unbedded, fine-grained quartzite.

The gneiss of the Blackhawk area is pervasively intruded by numerous masses of buff to light-gray, coarse-grained to pegmatitic, biotite-quartz-monzonite. Shapeless bodies of soft, black, medium-grained, quartz-plagioclase-amphibole rock (quartz-diorite?) up to 20 feet across are associated with these intrusive masses of quartz-monzonite near contacts with the gneiss. South of Surprise Spring and in the lower reaches of Voorhies and Blackhawk canyons the brown gneiss occurs as scattered, somewhat reconstituted xenoliths in massive quartz-monzonite. The quartz-monzonite in these places frequently contains crystals of orthoclase 1 to 2 cm in diameter that enclose numerous small biotite flakes. It is occasionally also gneissic, with segregated biotite flakes forming parallel, usually contorted, layers.

The gneiss in the Blackhawk area is lithologically more like the pre-Cambrian(?) Baldwin gneiss defined by Guillou (1953) than the Arrastre quartzite defined by Vaughan (1922). In its type locality about a mile south of the mouth of Arrastre Canyon the Arrastre is a massive, hard, black, medium- to very-coarse-grained, slightly foliated, quartz-orthoclase-hornblende gneiss intruded by brilliant pink epidote-bearing muscovite-biotite-quartz-monzonite pegmatite dikes and lenses 1 to 20 feet thick. On the basis of lithologic similarity, therefore, the gneiss in the Blackhawk area probably should be correlated with the more distant Baldwin gneiss rather than with the nearby Arrastre quartzite.

Furnace limestone (Cf)- An irregular strip of gray, coarsely-crystalline marble that has been thrust northward over gneiss closely parallels the western two-thirds of the southern edge of the Blackhawk area. This marble is best exposed on the upper slopes of Blackhawk Mountain and in the hills southwest of Terrace Springs. It usually forms smooth, rubbly, gray ridges with broad rounded crests, though where erosion is rapid it produces bold, jagged aretes and steep, mobile screes.

This rock consists principally of medium-gray, medium- to very-coarsely-crystalline marble which in many places is dolomitic. The dolomite usually occurs as grains distributed through the marble in concentrations ranging up to 100 percent. The marble commonly contains prisms and radiating fibers of tremolite, as much as 1 cm long in the most coarsely recrystallized zones. Other accessory minerals are chlorite, quartz, diopside, and garnet. The marble frequently has a

banded appearance due to variations in color and, sometimes, grain size. On the basis of a calcareous quartzite lense interbedded with the marble in upper Blackhawk Canyon Woodford and Harriss (1928, p. 269) interpreted this banding as relict bedding. Richmond (1954, p. 40), on the other hand, found that it does not parallel sedimentary bedding as indicated by chert, siltstone, and quartzite layers in the marble in the vicinity of Furnace Canyon. A few outcrops of the marble near Round Mountain are black, finely-crystalline, and fetid; this rock very strongly resembles the fossiliferous marbles in Furnace Canyon.

As a result of thrust-faulting the marble on Blackhawk Mountain and Round Mountain is pervasively shattered and in places brecciated, sometimes with rotation of individual fragments. Along faults the marble is usually much recrystallized and stained deep red by hematite and limonite. Most of the mines in the area are located on faults in the marble; the ore is the red, clayey, hematite-rich gouge, which carries some gold and silver.

Exposed in the core of an anticline south of the mouth of Grapevine Canyon is a sequence of light-gray, buff-weathering, fine- to medium-grained, crystalline dolomites and dolomitic marbles which is about 900 feet thick, assuming no hidden structural complications. At the base of this sequence are contorted beds of quartz-biotite schist and possibly quartzite which unfortunately have been almost engulfed by an igneous intrusion. The top of this sequence is separated from the common gray marble by a resistant, cliff-forming bed of pure white, finely-crystalline, sugary marble 10 feet thick which weathers to smooth, light-gray surfaces with distinctive white highlights on their corners and edges.

The marble on Blackhawk Mountain crops out with no lithologic change continuously westward 6 miles to Furnace Canyon, the type locality for the Furnace limestone defined by Vaughan (1922). All investigators have correlated the marble of the Blackhawk area with the marble of Furnace Canyon despite the fact that at least one major fault, the Helendale, transects this marble in Cushenbury Canyon, halfway between the two localities.

No fossils have been found in the Furnace limestone within the Blackhawk area; however, Woodford and Harriss (1928) and Richmond (1954) collected poorly preserved, metamorphosed, but nearly undistorted Mississippian fossils from the marble in the vicinity of Furnace Canyon.

Cactus granite (cqm, cqd)- Regularly jointed gray quartz-monzonite associated with minor amounts of easily weathered black quartz-diorite underlies most of the southern margin of the Blackhawk area. This rock is well-exposed in upper Grapevine Canyon and in Cactus Flat immediately south of it. It forms uneven buff-colored hills, steep sandy slopes, and huge rounded outcrops.

The quartz-monzonite is a uniformly buff to light-gray, coarse-grained, equigranular rock containing about 40 percent quartz, 30 percent plagioclase, 25 percent orthoclase, and 5 percent biotite. It intrudes the Furnace limestone over an extensive area south of Blackhawk Mountain, and it is very likely in part, if not wholly, the quartz-monzonite that is so widely intermingled with the biotite gneiss elsewhere in the Blackhawk area.

The quartz-diorite is a dark-gray to black, medium- to coarse-grained rock containing about 40 percent plagioclase, 25 percent horn-

blende, 20 percent biotite, and 15 percent quartz. It crops out along an irregular zone a few hundred feet wide between the Furnace limestone, which it intrudes, and the quartz-monzonite, which intrudes it.

Vaughan (1922, p. 365) gave the name Cactus granite to the quartz-monzonite and quartz-diorite in upper Grapevine Canyon and in the vicinity of Cactus Flat; Guillou (1953, p. 12) has suggested the more accurate term, "Cactus quartz-monzonite," for these rocks.

Hewett and Glass (1953, p. 1049) found by the uranium-lead method that a pegmatite associated with the Cactus granite about 15 miles east of Cactus Flat is approximately 155 million years old, or somewhat less if non-radiogenic lead is a significant constituent of the minerals analyzed. Thus, the Cactus granite was probably emplaced during the Jurassic or Cretaceous periods.

Younger rocks

The younger rocks of the Blackhawk area comprise fanglomerates and landslide breccias derived from the uplifted massif of the San Bernardino Mountains (tables 1 and 2). They are characterized by abrupt lithologic changes and numerous angular unconformities which reflect a complex history of contemporaneous deposition and deformation. Though they are doubtless late Tertiary and Quaternary in age, they cannot be certainly correlated with similar rocks elsewhere in the region because no fossils have been found in them.

Old Woman sandstone (To)- Small, patchy areas of massive reddish-buff conglomeratic arkose are exposed in many places along the lower slopes of Blackhawk Mountain from Surprise Spring to Arrastre Canyon. This sandstone is unique among the younger rocks because it is totally devoid of marble clasts. It is generally easily eroded and forms typical badlands topography. It is lithologically and stratigraphically identical to the "older desert deposits" reported by Vaughan (1922, p. 385) from near Cushenbury Springs west of the Blackhawk area and near Old Woman Springs east of it. This formation is herein named the Old Woman sandstone (a new name) and lower Blackhawk Canyon, the most extensive area of exposure, is designated the type locality. It is the oldest of the younger formations in the Blackhawk area.

Woodford and Harriss (1928, p. 274) and Richmond (1954, p. 124) correlated the Old Woman sandstone with the lithologically similar Rosamond series (Hershey, 1902, p. 365), a sequence of non-marine sedimentary, pyroclastic, and volcanic rocks exposed in the Rosamond Hills

in the western Mojave Desert. The name Rosamond has been applied to such a miscellaneous assemblage of Tertiary rocks in the Mojave Desert, however, that it has been rejected for use by the U. S. Geological Survey (Wilmarth, 1938, p. 1843). The name Tropico group is now applied to the original Rosamond near the type locality (Dibblee, 1958, p. 135). Inasmuch as no fossils have been found in the Old Woman sandstone, and it crops out over a limited area nearly 90 miles from the Rosamond Hills, correlation with the Tropico group (Rosamond series) appears questionable at best. For this reason the Old Woman sandstone is treated in this paper as a separate formation.

The Old Woman sandstone rests in depositional contact on deeply weathered gneiss. The ancient erosion surface on which the basal sandstone was deposited had at least 150 feet of relief. It probably resembled the present gneiss terrane south of Surprise Spring, as it is almost certainly a slightly tilted and recently exhumed remnant of the same erosion surface.

The Old Woman sandstone becomes finer-grained, more massive, and less conglomeratic stratigraphically upward and geographically northward. The coarser facies of the Old Woman sandstone, which is well-exposed near the Voorhies fault in Blackhawk Canyon, is a massive reddish-buff to red-brown conglomeratic arkose consisting of a matrix of uncemented, poorly sorted, coarse-grained, angular fragments of quartz, feldspar, hornblende, magnetite, biotite, and other dark minerals in which are embedded subrounded to subangular pebbles and scattered cobbles of vesicular andesite, gneiss, quartzite, schist, vein quartz, and rhyolite(?), in order of decreasing abundance.

All except the volcanic lithologies are exposed in the San Bernardino Mountains to the south. Clasts of marble are totally absent. A few resistant beds of coarse sandstone are partially cemented with calcite, but the arkose for the most part contains very little carbonate. Bedding in this rock is defined by thin layers of pebbles and by gradations in average grain size. Cross-bedding is rare, but where it does occur, it dips steeply northward between gently dipping bedding surfaces usually 1 to 3 feet apart. Filled channels are equally rare, and are usually small and inconspicuous.

The finer facies of the sandstone, which is best exposed near the mouth of Blackhawk Canyon, is a massive, practically unbedded yellowish-buff to brown arkosic mudstone composed of uncemented, slightly sorted, fine-to medium-grained fragments of quartz, feldspar, and weathered dark minerals. Interbedded with the mudstone are occasional beds 1 to 2 feet thick of poorly sorted, coarse-grained, calcareous sandstone, and of pebble conglomerate containing many subangular fragments of volcanic cinders and bombs and a few rounded clasts of gneiss and quartz-monzonite embedded in a fine-grained matrix. Calcareous concretions amoeboid in shape and 2 to 30 cm in diameter locally occur in the more massive mudstone and are usually distributed in planes parallel to the bedding. In the top 20 feet of the section and likewise roughly paralleling the bedding are discontinuous highly irregular layers 1 to 10 cm thick of a hard, white, aphanitic rock (tuff?) which forms sharp contacts with the enclosing mudstone. The mudstone contains no marble clasts and very little carbonate cement except within a few feet of the contact with the conformably overlying Member 1 of the carbonate-rich

Cushenbury Springs formation.

The Old Woman sandstone thins rapidly northward; in Blackhawk Canyon the thickness decreases from an estimated 600 feet near the Voorhies fault to a measured 200 feet near the mouth of the canyon 4500 feet to the north. In addition, bedding in the sandstone generally dips northward about 10 degrees more steeply than the contact with the underlying gneiss; and cross-bedding, which is surprisingly rare, always dips to the north. These structural and stratigraphic features together with the lithologic character of the Old Woman sandstone suggest that it was deposited as an alluvial fan northward from the primordial San Bernardino Mountains under arid conditions similar to those now existing in the Mojave Desert.

Cushenbury Springs formation (Qc)- A series of closely related landslide breccias and cobble fanglomerates derived almost wholly from the Furnace limestone underlies the bajada slope and lower foothills along the northern escarpment of the San Bernardino Mountains from Arrastre Canyon 12 miles west to Dry Canyon. These rocks are mostly covered by Recent fan gravels on the bajada slope, but are extensively exposed by erosion in the foothills, where they form gray to buff rubble-covered slopes with occasional aretes and talus chutes. These marble-bearing fanglomerates and breccias are herein named the Cushenbury Springs formation (a new name) after the springs near the mouth of Cushenbury Canyon. In the Blackhawk area the formation is divided into seven members (table 2) on the basis of lithology, stratigraphic relationships, and degree of deformation. The breccia members are further subdivided according to parent lithology. Typical ex-

TABLE 2

MEMBERS OF THE CUSHENBURY SPRINGS FORMATION

IN THE BLACKHAWK AREA

Member 7: Blackhawk breccia

Furnace limestone clasts (Qc7f)

Old Woman sandstone clasts (Qc7o)

gneiss clasts (Qc7g)

mixed clasts (Qc7m)

Member 6: fanglomerate (Qc6)

Member 5: landslide debris (Qc5)

Member 4: breccia

Furnace limestone clasts (Qc4f)

Old Woman sandstone clasts (Qc4o)

gneiss clasts (Qc4g)

mixed clasts (Qc4m)

Member 3: fanglomerate (Qc3)

Member 2: breccia

Furnace limestone clasts (Qc2f)

quartzite clasts (Qc2q)

Member 1: fanglomerate (Qc1)

Members are listed in order from youngest to oldest. Lithologic subdivisions are listed in order of decreasing importance. Parentheses enclose the appropriate map symbol.

amples of the fanglomerates and breccias of the Cushenbury Springs formation are well-exposed at the mouth of Blackhawk Canyon.

Vaughan (1922, p. 392) mapped the Cushenbury Springs formation as Heights fanglomerate, a formation he had defined on the south side of the San Bernardino Mountains, because the two "are probably of about the same age." Subsequently, Woodford and Harriss (1928, p. 279) adopted the name Blackhawk breccia for the fanglomerates and breccias of the Blackhawk area, but retained the name Heights fanglomerate for equivalent rocks near Cushenbury Springs. This paper restricts the name Blackhawk to the youngest breccia at Blackhawk Canyon in accordance with currently accepted informal geologic usage, and it discards the name Heights for the marble-bearing fanglomerates and breccias along the northern escarpment of the San Bernardino Mountains.

Member 1, the lowest member of the Cushenbury Springs formation in the Blackhawk area, is a limestone-cobble fanglomerate which rests conformably on the Old Woman sandstone. It is well-exposed in the canyon southwest of Surprise Spring, in middle Miles Canyon, and on the hill east of the mouth of Blackhawk Canyon, its type locality.

The contact between Member 1 and the underlying Old Woman sandstone is usually sharp, roughly planar, and locally channelled. Below it, the uppermost foot of sandstone contains a few rounded pebbles of marble less than 1 cm in diameter; whereas, above it, the lowermost foot of fanglomerate consists almost entirely of subrounded clasts of marble up to 20 cm in diameter. This contact clearly represents a significant episode in the geologic history of the Blackhawk area.

Near the mouth of Blackhawk Canyon Member 1 is at least 750 feet thick. It dips steeply northward and consists for the most part of well-cemented fanglomerate composed of practically unsorted subangular to subrounded pebbles, cobbles, and boulders of Furnace limestone, with cobbles predominating. Bedding is faintly defined by crudely sorted irregular pebble layers. The basal 10 to 15 feet of this unit consists of massive arkosic limestone-pebble conglomerate and conglomeratic sandstone containing pebbles of gneiss and vesicular andesite. Interbedded with the fanglomerate about 100 feet higher in the section is a 20-foot layer of marble breccia (similar to Member 7) with as much as 2 feet of gneiss breccia at its base. The upper contact of Member 1 in this locality is covered by Recent fan gravels.

Southwest of Surprise Spring Member 1 is up to 40 feet thick. It consists of 6 to 10 feet of limestone-cobble fanglomerate overlain by a maximum of 30 feet of arkosic mudstone containing scattered rounded pebbles of marble. Member 2 rests in angular unconformity on both Member 1 and the Old Woman sandstone in this locality.

In upper Miles Canyon Member 1 is probably in excess of 50 feet thick. It consists of 25 feet of resistant limestone-cobble fanglomerate overlain by 25 feet of marble-bearing arkosic sandstone. Both Member 1 and the Old Woman sandstone in this locality pinch out against the sloping surface of the gneiss on which they were deposited. An unidentified gneiss breccia, possibly a fault slice, rests on Member 1.

Member 2 of the Cushenbury Springs formation is a resistant gray marble breccia which mantles the northwest slopes of Blackhawk Mountain from Del Mar Flat, its type locality, westward nearly to Cushenbury

Canyon. In addition, it is exposed in Blackhawk Canyon. Except for a small area of calcite-cemented quartzite breccia 1000 feet southeast of Surprise Spring, Member 2 is composed entirely of angular clasts of Furnace limestone. Nearly all of the member is unsorted and unstratified landslide debris, but faint bedding revealed by weathering in the cliff-face on the west side of Del Mar Flat suggests that it may contain talus deposits. Member 2 probably has a thickness of more than 250 feet just west of Del Mar Flat. It thins to the north, and pinches out under Member 3 north of Surprise Spring.

Member 3 is a flat-lying well-cemented brown limestone-cobble fanglomerate mainly derived from Member 2 which forms much of the alluvial surface northwest of Surprise Spring. It is composed of poorly sorted, roughly stratified, rounded to subrounded pebbles and cobbles of Furnace limestone. At the head of the alluvial slope an unknown thickness of Member 3 rests on Member 2. In the low hills a mile to the north it rests in slight angular unconformity on Old Woman sandstone and has a thickness of about 100 feet (which probably includes at its base a few feet of Member 1). A mile farther to the north it rests conformably on Old Woman sandstone and has a thickness of only 20 feet. Member 3 probably underlies most of the alluvial slope northeast of Blackhawk Mountain.

Member 4 of the Cushenbury Springs formation is completely analogous to Member 7, the Blackhawk breccia. It composes a landslide lobe 3 miles long by 2 miles wide, now dissected by erosion and partly buried by alluvium, which formerly extended down the alluvial slope from the mouths of Miles and Voorhies canyons to Akron Hill, its type

locality. In addition it crops out in upper Miles Canyon and on the north side of Round Mountain. Lithologically Member 4 is identical to Member 7 except that it is completely recemented.

Member 4 rests on Old Woman sandstone at Akron Hill and on limestone-cobble fanglomerate, probably Member 3, a mile to the east at the Akron Silver Reef mine. It is overlain by Member 6 in Miles Canyon and near Old Woman Peak, and by Member 7 northwest of Akron Hill.

Member 5 consists of landslide debris which covers the north wall of Grapevine Canyon, its type locality, for a distance of more than one-half mile upstream from the canyon mouth. It is composed principally of large masses of Furnace limestone which slipped southward down the flank of Blackhawk Mountain into lower Grapevine Canyon, as shown by a series of small closed depressions and traces of fissures located 700 feet above the canyon floor. Member 5 formerly filled the canyon to a depth of several hundred feet, as indicated by remnants of fan gravel, probably correlative with Member 6, perched 400 feet above the present streambed.

Member 6 is a light-brown limestone-pebble fanglomerate which composes the remains of an extensive alluvial fan resting on Member 4 in Miles Canyon, its type locality. It is also represented by smaller fans built on Member 4 south of Old Woman Peak and probably by remnants of fan gravel resting on Member 5 in lower Grapevine Canyon. It forms smooth surfaced, round crested, buff-colored hills with very few outcrops except in road cuts. Member 6 consists of nearly unsorted angular to subrounded pebbles and occasional cobbles in a matrix of coarse arkosic sandstone. The clasts consist 95 percent of marble and 5 percent

of gneiss, volcanic rocks, and quartzite, in order of decreasing abundance.

Member 7, the Blackhawk breccia, is the youngest member of the Cushenbury Springs formation in the Blackhawk area. It composes the great landslide lobe, herein termed the Blackhawk slide, that extends down the alluvial slope from the mouth of Blackhawk Canyon, its type locality. In addition it is exposed along the west side of lower Blackhawk Canyon, in upper Blackhawk Canyon, and in lower Voorhies Canyon.

The Blackhawk slide increases in thickness from about 30 feet at the proximal end near the mouth of Blackhawk Canyon to a maximum of nearly 100 feet at the distal end north of Hill 3747. It involves 10 billion cubic feet, or about 700 million tons, of crushed marble. The slide has a hummocky surface little affected by erosion except near the distal edge and along the two main drainage channels which cross it. The proximal half of the slide has been partly buried by Recent fan gravels discharged from Blackhawk Canyon.

Member 7 consists almost entirely of gray unsorted and unstratified breccia of fresh angular fragments of Furnace marble ranging in size from powder up to 25 cm in diameter, with most clasts being about 2.5 cm in diameter. Occasional large boulders of Member 2 (Qc2f) occur in the breccia, the largest observed being 35 by 20 by 15 feet above the surface. In addition a few boulders of quartzite breccia from Member 2 (Qc2q) are associated with clasts of marble breccia (Qc2f) and quartz-monzonite near the distal end of the Blackhawk slide. Cementation of Member 7 has not progressed nearly so far as in the older mem-

bers of the Cushenbury Springs formation; only the surficial 10 to 15 feet of the breccia is well-indurated, forming a distinctive rim at the crests of steep slopes.

Around the distal end and along the west edge of the Blackhawk slide is a discontinuous strip less than 100 feet wide of completely disaggregated Old Woman sandstone associated with minor amounts of gneiss breccia. This sandstone "breccia" is distinguished from undisturbed sandstone on the basis of three criteria: (a) vesicular andesite clasts in it are invariably crushed and smeared out, (b) bedding is never recognizable, and (c) marble breccia is occasionally mixed with it. The contacts between the sandstone "breccia" and the marble breccia are always sharp and usually marked by a thin layer of green, clayey gouge. The presence of Member 3 underlying Member 7 (both Qc7f and Qc7o) 2 miles north of Surprise Spring demonstrates that the sandstone "breccia," rather than being bulldozed up locally, was carried at least 4 miles northward by the Blackhawk slide.

In upper Blackhawk Canyon Member 7 consists in part of light-gray to brown "mixed breccia" composed mainly of disintegrated gneiss containing a liberal admixture of crushed Furnace limestone and disaggregated Old Woman sandstone. The contacts of this "mixed breccia" with the other units of Member 7 are generally gradational over a distance of a few feet.

The sandstone "breccia," gneiss breccia, and "mixed breccia" are minor constituents of the essentially monolithologic marble breccia of Member 7.

Recent fan gravels (Qf) and minor landslides (Qs)- Recent fan gravels form most of the alluvial slope that comprises the northern three-fourths of the Blackhawk area. They consist of material that is indistinguishable, except by its lack of consolidation, from the older fanglomerates. The clasts composing this material become smaller and rounder to the north, and the proportion of marble fragments decreases. In an extensive area north of Old Woman Peak a mantle of locally derived alluvium only a few feet thick covers a deeply weathered surface of gneiss; this may be a true pediment surface.

Minor landslides up to 1000 feet in maximum dimension have occurred in three places in the Blackhawk area where erosion undermined Furnace limestone or massive marble breccia. These landslides are located in lower Grapevine Canyon, in Miles Canyon, and in the canyon southwest of Surprise Spring. They involved large masses of rock moving as a unit on a slip-surface and forming a well-defined scar and lobe. Talus deposits, though they are extensively developed on Blackhawk Mountain, were not mapped.

Faults and folds

The faults and folds of the Blackhawk area fall chronologically into six groups: (a) the northwest-trending right-lateral Lester fault, oldest in the area, (b) the south-dipping Santa Fe thrust zone, and the southwest-dipping Round Mountain and Terrace Springs thrust-faults, (c) the north-dipping Mill and Hill 3747 reverse faults and associated minor monoclinal folds, (d) the northwest-trending Blackhawk and Grapevine folds, (e) the northeast-trending left-lateral Blackhawk fault, and (f) the northwest-trending Silver Reef fault, youngest in the area, which is related to the Helendale and Old Woman Springs faults, major structural features west and east of the area, respectively. All of the faults of the Blackhawk area, except possibly the Lester fault, are younger than the Old Woman sandstone.

Noteworthy among the minor structural features of the Blackhawk area are small closed depressions and fissures near the summit of Blackhawk Mountain, evidently formed during the great rockfall that produced the Blackhawk breccia.

Lester fault- The Lester fault is a vertical zone of shearing and recrystallization more than 100 feet wide which cuts northwesterly through the Furnace limestone on the ridge north of lower Grapevine Canyon. Drag folds and slickensides suggest that the northeast block moved relatively down and to the right. The Lester fault is truncated by the Santa Fe fault at its northwest end in upper Miles Canyon, and is covered by Recent fan gravels at its southeast end near the Lester mine.

Santa Fe thrust zone- The Santa Fe thrust zone comprises the south-dipping belt of sheared gneiss and Furnace limestone which lies between the Voorhies and Grapevine thrust-faults on Blackhawk Mountain.

The Voorhies fault, the lowest in the thrust zone, dips south 20 to 40 degrees. Along it, in Blackhawk Canyon, gneiss has been thrust 1000 feet over Old Woman sandstone. The fault is marked by a few inches of clayey green gouge and by shearing in the gneiss, whose foliation roughly parallels the fault surface. In Voorhies Canyon the fault consists of a shear zone in the gneiss several feet wide. In upper Miles Canyon, gneiss, Old Woman sandstone, and Member 1 of the Cushenbury Springs formation are thrust about 50 feet over Old Woman sandstone. At its eastern end in upper Miles Canyon the Voorhies fault probably joins the Santa Fe fault; at its western end in Blackhawk Canyon it is covered by Members 2 and 7 of the Cushenbury Springs formation. The Voorhies fault is thus older than Member 2 and younger than, or contemporaneous with, Member 1.

Between the Voorhies and Santa Fe faults, two subsidiary thrust-faults are usually distinguished as 3- to 4-foot shear zones in the gneiss. In upper Blackhawk Canyon, however, a wedge of Old Woman sandstone about 4 feet thick is exposed beneath the lower fault, and a similar wedge less than 20 feet thick of somewhat sheared limestone-cobble fanglomerate, probably Member 1, is exposed under the upper fault. Both faults die out to the east in upper Voorhies Canyon; they are covered by Members 2 and 7 to the west in Blackhawk Canyon.

The Santa Fe fault, along which Furnace limestone has been thrust

over gneiss, Old Woman sandstone, and Member 1 fanglomerate, is the principal break in the Santa Fe thrust zone. At the Santa Fe mine above Blackhawk Canyon the usually massive gray marble is sheared, recrystallized, bleached, and reddened by hematite for a distance of over 200 feet above the fault surface. At the fault itself is a zone 30 feet thick of brecciated marble and gold- and silver-bearing clayey red gouge. The gneiss below the fault is sheared and thoroughly fractured. The zone of red hematite stain and recrystallization diminishes in thickness eastward; it is less than 100 feet thick in upper Miles Canyon. The Santa Fe fault is covered by Members 2 and 7 to the west in Del Mar Flat. Thus it, like the Voorhies fault, is older than Member 2 and younger than, or contemporaneous with, Member 1.

In Miles Canyon the Santa Fe fault surface is folded so that its trace turns northward down the east wall of the canyon and disappears beneath the breccia of Member 4. This interpretation is based on inference rather than observation, because the critical relationships in upper Miles Canyon are masked by landslides. The alternative interpretation is that the fault exposed near the lower end of Miles Canyon, which dips east 50 degrees and separates marble on the east from sandstone on the west, is a cross-fault that displaces the Santa Fe fault at least 3000 feet northward and downward on the east. The fold hypothesis is preferred to the cross-fault hypothesis for the following reasons: (a) there is no apparent offset and no discoverable fault zone in the Cactus granite on the logical southward extension of the fault in lower Miles Canyon, (b) no offset western extension of the Lester fault, which could hardly be overlooked, crosses Blackhawk Mountain, and (c) "unfolding" of the

observed fault segment in lower Miles Canyon on the basis of dips in the Old Woman sandstone leads to an original dip of about 30 degrees to the south for this fault, which is in accordance with the undisturbed attitude of the Santa Fe fault. The folding also affected the Lester fault, which must originally have been a right-lateral normal fault dipping northeast (assuming no previous deformation of the fault surface).

The Grapevine fault, which traverses the Furnace limestone on the south slopes of Blackhawk Mountain, dips south 40 to 60 degrees and consists of a hematite-stained, recrystallized, and slickensided zone 1 to 10 feet wide. Drag folds and slickensides uniformly suggest a left-lateral component of slip equal to the thrust component on this fault. According to Guillou (1953, p. 15) the Grapevine fault terminates against the younger Helendale fault to the west in Cushenbury Canyon. To the east it passes beneath the landslide debris of Member 5 and then under the Recent stream gravels in lower Grapevine Canyon. Because of the contrast in lithology of the Furnace limestone on opposite sides of the canyon in this vicinity it can be inferred that the fault follows the canyon as it curves to the north, and, therefore, that it must be folded in the same way, though possibly not as much, as the Santa Fe fault.

Round Mountain and Terrace Springs faults- On the northeast side of Round Mountain, shearing, brecciation, recrystallization, and red hematite stain in the Furnace limestone indicate the presence of a major fault that dips southwest approximately 30 degrees. This is the Round Mountain fault. Old Woman sandstone cropping out in a roadcut 50 feet downslope from the lowest marble outcrop demonstrates that it is a thrust-fault. The Round Mountain fault is covered by the breccia of

Member 4 north of Round Mountain and by Recent fan gravels east of it.

Extending southeast from Terrace Springs to Arrastre Canyon is a zone of sheared gneiss bounded by two reverse faults, the Terrace Springs faults, which dip southwest 50 degrees. Gneiss rests on Old Woman sandstone along the northern fault, and Furnace limestone intruded by Cactus granite rests on gneiss along the southern fault. Terrace Springs, and several other springs and seeps, rise along the southern fault. The Lester mill is built on the Recent scarp of a branch of this fault. To the northwest the Terrace Springs faults are covered by Recent fan gravels and by fanglomerate (probably Member 3) of the Cushenbury Springs formation. To the southeast they disappear beneath the stream gravels of Arrastre Canyon.

Blackhawk monocline and Grapevine folds- On the ridge between Blackhawk and Voorhies canyons the Old Woman sandstone dips north with an inclination of 10 degrees, probably near the angle of deposition. To the north, on the south side of the hill east of the mouth of Blackhawk Canyon, both the Old Woman sandstone and the overlying Member 1 fanglomerate dip 85 degrees to the northeast. Farther north, on the north side of the hill, the fanglomerate dips only 75 degrees to the northeast. Thus, the Old Woman sandstone and the Member 1 fanglomerate are monoclinally folded at the mouth of Blackhawk Canyon, forming a northwest-trending structural step approximately 1500 feet high. This is the Blackhawk monocline.

Attitudes of bedding in the Old Woman sandstone southwest of Surprise Spring suggest that the height and steepness of the monocline de-

crease northwestward from Blackhawk Canyon. Steeply dipping bedding in the sandstone in Miles Canyon indicates that the axis of the monocline trends southeast from the mouth of Blackhawk Canyon to lower Miles Canyon where it turns south toward the Lester mine.

A consequence of this interpretation is that the Round Mountain fault must be the eastward extension of the folded Santa Fe fault. An alternative interpretation is that the Blackhawk monocline is essentially a drag-fold on the Round Mountain fault, which continues straight northwest along the head of the alluvial slope and cuts off the drag-folded Santa Fe fault under the alluvial cover about 1000 feet northwest of the mouth of Miles Canyon. This interpretation is rejected because it requires at least 10 000 feet of thrust-slip, and therefore 5000 feet of vertical uplift, on the Round Mountain fault, which in turn necessitates the unlikely circumstance that the Old Woman sandstone is at least 4000 feet thick beneath Round Mountain. Because none of the evidence linking the Round Mountain to the Santa Fe fault is independent of these somewhat circumstantial structural arguments, however, they are treated separately in this paper.

The Grapevine folds, an open anticline and a tight syncline in the Furnace limestone that trend southeast from the mouth of Grapevine Canyon, may be the continuation of the Blackhawk monocline; but, in the absence of information on possible pre-existing folds in the limestone, they are treated as separate structural features. In this connection it should be mentioned that the evidently complex structure buried beneath the fan gravels between Round Mountain and Terrace Springs cannot be

satisfactorily inferred from any of the structural interpretations discussed here.

Mill and Hill 3747 faults- The Mill and Hill 3747 faults are anomalous because they are reverse faults that dip north.

The Mill fault is a few hundred feet north of the Blackhawk mill in Blackhawk Canyon. It dips north 55 degrees near the bottom of the canyon but steepens to 75 degrees 300 feet to the west where it passes under the breccia of Member 7. The fault has 200 feet of reverse-slip and, judging from slickensides, an equal amount of right-lateral-slip in this locality, gneiss being pushed over Old Woman sandstone. Reverse dips in the sandstone near the fault suggest an open drag-fold. To the east the Mill fault is displaced 800 feet northward by the Blackhawk fault. It appears east of this fault as a steeply-dipping 1-foot gouge zone in the gneiss, and farther east disappears beneath fan gravels at the mouth of Voorhies Canyon.

An unnamed fault, which may be conjugate to the Mill fault, trends northward along the west side of lower Blackhawk Canyon, then turns northwest under the Member 7 breccia. It is a reverse fault that dips steeply west and displaces gneiss over Old Woman sandstone. It frays out in the gneiss to the south without reaching the Mill fault. A minor branch of this fault displaces Old Woman sandstone a few feet northward over Member 2 breccia and Member 3 (?) fanglomerate at the mouth of Blackhawk Canyon.

The Hill 3747 fault dips north 75 degrees and is marked by a shear zone 50 to 100 feet wide traversing the gneiss 2500 feet northeast of Hill

3747. This fault evidently turns southwest under the Blackhawk breccia, which it does not deform, then west beneath the line of low anticlinal hills of Old Woman sandstone and Member 3 fanglomerate 1.5 miles northwest of Surprise Spring. Several angular unconformities in the fanglomerate suggest repeated deformation during, as well as after, deposition of Member 3.

A mile north of these hills Old Woman sandstone and Member 3 fanglomerate dipping northeast 40 degrees suggest a buried northwest-trending fault conjugate to the Hill 3747 fault.

Blackhawk fault- The Blackhawk fault follows the east side of Blackhawk Canyon from the head of the alluvial slope to the summit of Blackhawk Mountain. It dips eastward 50 to 65 degrees, has approximately 800 feet of left-lateral and 400 feet of reverse slip, and offsets the Mill fault and the faults of the Santa Fe thrust zone. Near the mouth of Blackhawk Canyon it brings sandstone dipping 90 degrees against sandstone dipping 40 degrees. In the gneiss north of the Blackhawk mill the fault is marked by 1 to 3 feet of clayey gouge. Immediately south of the Blackhawk mill, where it brings gneiss on the east over Old Woman sandstone on the west, it is 100 percent exposed for more than a quarter of a mile and consists of several anastomosing breaks. On Blackhawk Mountain it is characterized by a 1- to 2-foot red-stained, recrystallized, and slickensided zone in the Furnace limestone. The Blackhawk fault is covered by Member 7 breccia at the head of the alluvial slope and in upper Blackhawk Canyon.

The amount and direction of slip on the Blackhawk fault is ascertained by construction of two structure sections, one on each side of the

fault (fig. 3). Consider first the east section. (a) The monoclinal fold is reconstructed by projecting the base of the sandstone northward above the gneiss surface, then curving it downward to meet the ground at 85 degrees, and finally leveling it out in accordance with the decreasing dips in the fanglomerate of Member 1. The fact that the sandstone is exposed on Akron Hill and north of Surprise Spring means that it cannot be buried very deeply beneath the surface of the alluvial slope. (b) The thrust-slip on the Voorhies fault is found to be approximately 1000 feet by projecting the base of the sandstone northward from the wedge exposed beneath the lower subsidiary fault. (c) Erosion of the Old Woman sandstone south of the Voorhies fault prior to the deposition of Member 1 and the small, if any, movement on the Voorhies fault in Blackhawk Canyon subsequent to deposition of Member 1 are inferred by projecting the base of the fanglomerate northward from the wedge beneath the upper subsidiary fault. Consider now the west section. (a) Because it displaces the monoclinal fold, which is younger than the Voorhies fault, the Blackhawk fault must be younger than the Voorhies fault. (b) Because it does not displace the trace of the Voorhies fault more than 200 feet northeast on the west, the Blackhawk fault necessarily must have a left-lateral component of slip of at least twice the reverse component. (c) The Voorhies fault must cross the bottom of Blackhawk Canyon between the spring at the 5100-foot contour and the outcrop of Old Woman sandstone at the 5250-foot contour 400 feet to the south. (d) The elevation of the base of the sandstone north of the Voorhies fault, and hence the amount of reverse slip on both the Blackhawk (400 feet) and the Mill (200 feet) faults, is inferred

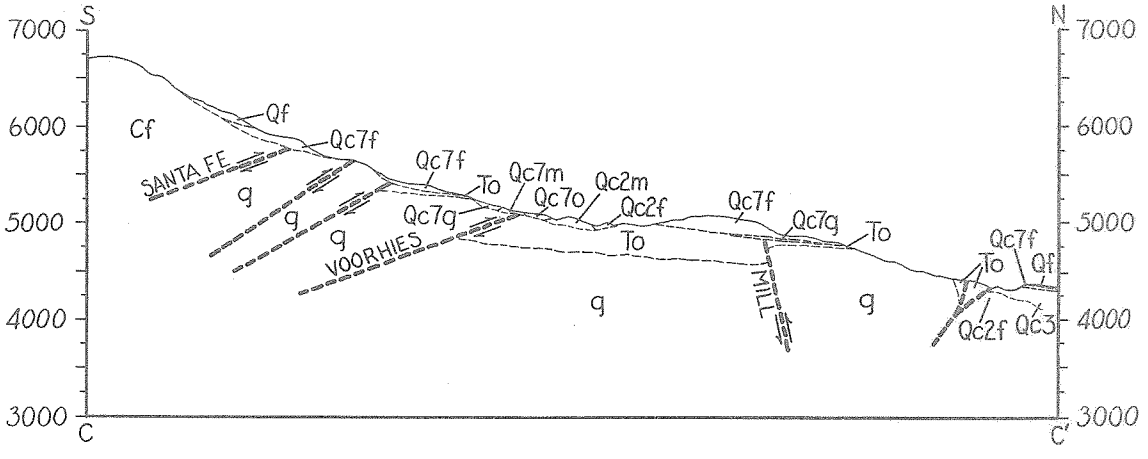

STRUCTURE SECTION ALONG WEST SIDE OF BLACKHAWK CANYON

STRUCTURE SECTION ALONG EAST SIDE OF BLACKHAWK CANYON

2000 0 2000 4000 6000 feet

FIGURE 3

STRUCTURE SECTIONS IN BLACKHAWK CANYON

by projecting the base of the sandstone northward from the outcrop at the 5250-foot contour to the Voorhies fault, then offsetting it diagonally downward 1000 feet along the fault. (e) The amount of left-lateral slip on the Blackhawk fault, and hence the place at which the Voorhies fault crosses Blackhawk Canyon, is determined from the apparent horizontal offsets of the Mill, Santa Fe, and Grapevine faults to be about 800 feet, assuming 400 feet of reverse slip on the Blackhawk fault. As might be expected, the Voorhies fault crosses Blackhawk Canyon at the spring. This analysis does not adequately explain the structure at the mouth of Blackhawk Canyon. The attitude of the beds in the narrow triangular block of Old Woman sandstone bounded by faults on the east, north, and west suggest that it was not displaced northward at all, or else was shoved southward about 800 feet after movement ceased on the Blackhawk fault.

An unnamed northeast-trending left-lateral reverse fault, analogous to the Blackhawk fault, has displaced gneiss over Old Woman sandstone and Old Woman sandstone over Member 2 breccia southwest of Surprise Spring; this suggests that the Blackhawk fault may be younger than Member 2.

Silver Reef fault- The Silver Reef fault is marked by a 10-foot, northeast-facing scarp of limestone-cobble fanglomerate, probably Member 3, east of the Akron Silver Reef mine, and by lower, east-facing scarps of gneiss west of Old Woman Peak. An unnamed fault characterized by a 30-foot, northeast-facing scarp of fanglomerate traverses the alluvial slope about a mile north of the mouth of Arrastre Canyon. Both these faults are doubtless Recent in age and related to

the Helendale and Old Woman Springs faults, which are much larger breaks of similar type west and east of the area, respectively.

Blackhawk Mountain fissures- Several small, elongate closed depressions and numerous drainage lines run transverse to the general slope on the summit ridge south of Del Mar Flat. They closely parallel the escarpment from which the breccia fell and strikingly resemble both in pattern and in scale the network of fissures formed in the limestone on Turtle Mountain during the Frank landslide of 1903 (Daly, Miller, and Rice, 1912, p. 17). They are, therefore, considered to be the traces of fissures which opened during the great rockfall that produced the Blackhawk breccia.

Similar features delineate the head of the Member 5 landslide in lower Grapevine Canyon; but apparently none remain from the rockfall that produced the Member 4 breccia.

Geologic history

The last chapter in the geologic history of the Blackhawk area, which embraces the sequence of events leading to the formation of the Blackhawk breccia, begins just before deposition of the Old Woman sandstone, when a terrain of moderate relief had developed on deeply weathered gneiss, quartzite, and quartz-monzonite. Limestone, however, probably was not yet exposed within or immediately south of the Blackhawk area.

Uplift- At this time, probably late in the Pliocene epoch, uplift and volcanic activity began south of the area. An extensive alluvial apron several hundred feet thick, the Old Woman sandstone, was built northward from the rising mountain mass. Uplift of Blackhawk Mountain then began with faulting on the Santa Fe thrust zone; and the Old Woman sandstone was partially stripped from the upraised block. Continued uplift and erosion then rapidly exposed the Furance marble, initiating deposition of the Member 1 fanglomerate of the Cushenbury Springs formation. When the fanglomerate had attained a thickness of about 100 feet, the first of the monolithologic landslides of the Blackhawk area occurred; a sheet of marble and gneiss breccia 20 feet thick slid at least a mile down the ancient alluvial slope, and was soon buried by the accumulating fanglomerate.

By the time Member 1 had become about 750 feet thick, activity in the Santa Fe thrust zone had ceased entirely. Then deformation along the northwest-trending Blackhawk monocline began, folding the west-trending Santa Fe thrust zone, the Old Woman sandstone, and the Member 1 fanglomerate, and completing uplift of Blackhawk Mountain.

Erosion and landsliding- Erosion of the uplifted unresistant Old Woman sandstone on the northwest slopes of Blackhawk Mountain soon undermined the overthrust Furnace limestone (and also, evidently, the quartzite) near the crest, causing the landslide which deposited the Member 2 breccia over several square miles in the western part of the area. Deposition of the Member 3 fanglomerate then began on the alluvial slope to the north; concurrently, activity on the Hill 3747 fault produced an anticline and minor unconformities in Member 3 north of Surprise Spring. The Mill fault was active at this time.

In a similar manner erosion of the Old Woman sandstone on the northeast slopes of Blackhawk Mountain subsequently led to the Member 4 landslide. At about the same time sliding occurred in Grapevine Canyon (Member 5), filling it to a depth of several hundred feet. The Blackhawk fault was active during this period. Deposition of the Member 6 fanglomerate, an alluvial fan that mantled the northeast slopes of Blackhawk Mountain to an elevation of 5500 feet, immediately followed the Member 4 landslide. Minor fans were built on Member 4 near Old Woman Peak, and on Member 5 in Grapevine Canyon. At about this time the Silver Reef fault was active in the vicinity of the Akron Silver Reef mine.

Once again erosion of the unresistant younger rocks on the north slope of Blackhawk Mountain undermined the Furnace limestone, this time at the summit itself. The result was deposition of the Blackhawk breccia by a landslide even greater than those which had occurred earlier. Since then erosion has continued on Blackhawk Mountain; but, because Old Woman sandstone no longer underlies the Furnace limestone

near the crest of the mountain, it is unlikely that another great landslide will ever occur in the Blackhawk area.

MECHANICS OF THE BLACKHAWK SLIDE

Introduction

The geological evidence demonstrates that the Blackhawk slide, herein defined as that portion of the Blackhawk breccia (Member 7) mantling the alluvial slope northward from Blackhawk Canyon, was deposited not as a slow-moving mudflow but as a nearly nondeforming sheet of breccia that traversed the gently inclined alluvial slope at high speed. Mechanical considerations suggest the hypothesis that the breccia sheet slid on a layer of compressed air, much as the slipper in a thrust-bearing slides on a film of oil. This hypothesis explains the origin of all the major features of the slide. Theoretical analysis of the flow in the lubricating air layer supports the air-lubrication hypothesis for the Blackhawk slide.

Symbols- All of the symbols used in this paper, except the usual mathematical symbols, are defined in the following summary. The standard notation of fluid mechanics is used wherever possible. The numbers in parentheses refer to the equation in which the symbol is first used.

A	Constant of integration, (18).
B	Dimensionless parameter, (19c).
b	Thickness of the breccia sheet, (1a).
c_v, c_p	Heat capacity of fluid at constant volume and constant pressure, respectively, (2d).
F	Dimensionless parameter, (22a).
G	Dimensionless function of velocity profile, (22b).

g	Acceleration due to gravity, (1a).
H	Dimensionless function of h, (22c).
h	Clearance, or thickness of air layer, (1a).
K	Molecular thermal conductivity of fluid, (2c).
k	Permeability of breccia, (29a).
ℓ	"Mixing-length," (16).
m	$m = 1/\gamma$, (6b).
n	$n = 2/(3m + 1)$, (30).
p	Fluid pressure, (2b).
Q	Net mass flux at a cross-section, (1c).
q	Volume flux of air up through breccia, (28).
R	Reynolds number, (8e).
S	Drag function, (23a).
T	Averaging period, (3a).
t	Time, (1a).
$\underline{u}$	Velocity of fluid, (2a).
$\underline{\tilde{u}}$	Fluctuation velocity, (3b).
$\underline{U}$	Mean velocity, (3a).
U_s	Velocity of breccia, (1e).
$\tilde{u}, \tilde{v}$	x- and y-components of fluctuation velocity, (7b).
U, V	x- and y-components of mean velocity, (7a).
$\underline{X}$	Body force on fluid, (2b).
x, y, t	Cartesian co-ordinates of point, (1a).
α, β	Dummy variables of integration, (22b).
γ	Ratio of heat capacity at constant pressure to heat capacity at constant volume, (6a).

θ Absolute temperature of fluid, (2d).

κ Prandtl's "universal constant," (17).

λ A measure of boundary roughness, (17).

μ Molecular viscosity of the fluid, (2b).

ρ Density of fluid, (2a).

τ Shear stress, (23a).

Φ Dissipation function, (2c).

ψ Angle of inclination of the alluvial slope, (25).

sgn ϕ A function which is +1 for $\phi > 0$, 0 for $\phi = 0$, and -1 for $\phi < 0$, (16).

Physical features

The Blackhawk slide has many distinctive and well-preserved physical features, from which information can be obtained that leads to the hypothesis that the Blackhawk slide descended the gently inclined alluvial slope as an essentially nondeforming sheet of breccia sliding at high speed on a cushion of compressed air.

Form and size- In plan the Blackhawk slide is a narrow, symmetrical lobe with an overall length of almost 5 miles, an average width of about 1.5 miles, and a maximum width of nearly 2 miles. It descends from an elevation of 4500 feet at its proximal end near the mouth of Blackhawk Canyon (approximately 2000 feet below and 6000 feet north of its source on Blackhawk Mountain) to an elevation of 3100 feet at its distal end near the floor of Lucerne Valley. Its thickness, which is quite regular except along the lateral edges and in the vicinity of Hill 3747, varies uniformly from a measured 30 feet near the proximal end to an estimated 100 feet near the distal end (Figure 4). The volume of the slide is, therefore, about 10^{10} cubic feet.

The lateral edges of the proximal 3 miles of the Blackhawk slide are delineated by straight, narrow ridges of breccia which rise 50 to 100 feet above the surrounding terrain (Figure 1). In places the major lateral ridge is accompanied, usually on its interior side, by parallel subsidiary ridges. A similar lateral ridge, now much subdued by erosion, marks the partially exposed east edge of the Member 4 slide.

The edge of the distal 2 miles of the Blackhawk slide is bounded by a somewhat sinuous, slightly dissected scarp about 50 feet high (Figure 1). The summit of this scarp usually rises a few feet above the

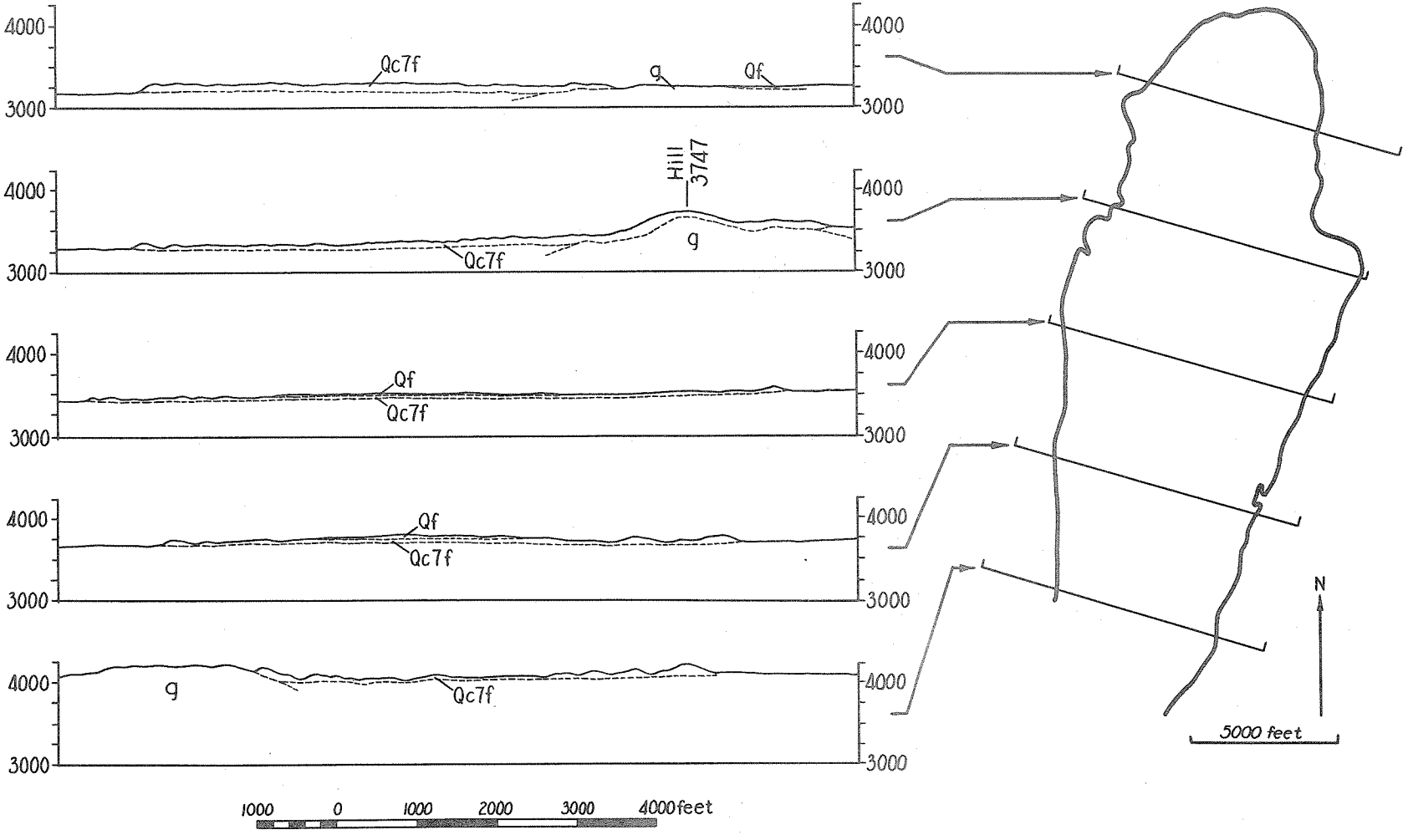

FIGURE 4

TRANSVERSE CROSS-SECTIONS THROUGH THE BLACKHAWK SLIDE

FIGURE 5

TOPOGRAPHIC TEXTURE OF THE BLACKHAWK SLIDE

Vertical air photo of northern half of Blackhawk slide. Hill 3747 at lower right. Light-colored areas are playas in closed depressions. (Photo by U. S. Department of Agriculture, 12 February 1953.)

local level of the slide surface, thus forming an irregular low rim behind which numerous small playas have developed. The distal edge of the Member 4 slide is bounded by a similar low rim and scarp.

The surface of the Blackhawk slide is characterized by low rounded hills and small closed basins with about 10 to 30 feet of local relief. Drainage channels, though numerous, are small and disorganized except adjacent to the few main channels crossing the slide. The topography of the slide has a definite fabric (Figure 5); near the distal end the elongate hills and basins tend to lie at right angles to the axis of the slide, and at the proximal end they appear to curve northward on each side so as to meet the lateral ridges tangentially.

The higher hills on the Blackhawk slide probably reflect underlying gneiss knobs which projected above the former alluvial surface. The most prominent of these is Hill 3747, a steep-sided, round-topped eminence situated at the west end of a breccia-mantled gneiss ridge that rises more than 200 feet above the general level of the slide surface. The thickness of the breccia mantle is unknown, but is probably less than 50 feet along the crest of the ridge.

The motion of the breccia in a zone 1500 feet wide along the eastern edge of the Blackhawk slide was prematurely terminated by the Hill 3747 ridge. Though the sliding breccia overtopped Hill 3747, it travelled only a few hundred feet down the distal side of the hill before coming to rest; and the easternmost 500 feet of breccia stopped even before reaching the crest of the ridge. The subparallel ridges of breccia on the western and southwestern slopes of Hill 3747 (Figure 5) doubtless are lateral ridges that were successively formed and abandoned as the unimpeded middle region of the slide adjusted to the arrested motion of the breccia

ascending the hill.

Structure and composition- The Blackhawk breccia is composed almost exclusively of crushed Furnace limestone. The individual fragments are roughly equant, and range in size from powder to about 25 cm, with the modal diameter being approximately 2.5 cm. A few exceptionally large blocks, invariably composed of the well-cemented Member 2 breccia, range up to 35 feet in maximum dimension.

The size distribution of the clasts, as determined by measurements made at eight localities, does not significantly vary from place to place on the slide (Figure 6). At each locality 225 clasts, representing an exposed surface area of about 40 square feet, were selected for measurement by means of a 5-inch square-mesh grid laid against the outcrop. All of the counts were made on vertical weathered faces near the upper surface of slide. Relative to the usual mechanical analysis, this method discriminates against the smaller sizes, because it determines the number of clasts per unit volume that fall in a given grade. Moreover, the smaller particles are more easily weathered from the outcrop. On the other hand, it is a fast, convenient method of comparing the relative magnitudes of the larger size grades in different samples.

In many places the Blackhawk breccia contains roughly lenticular (though sometimes contorted) zones up to 20 feet across composed entirely of a single distinctive variety of marble. The clasts in these zones are often loosely fitted together as in a three-dimensional jigsaw puzzle, so that color bands, for example, often continue from clast to clast without significant offset, thus suggesting single large blocks fractured by impact, and subsequently not much deformed. The heterogeneous transi-

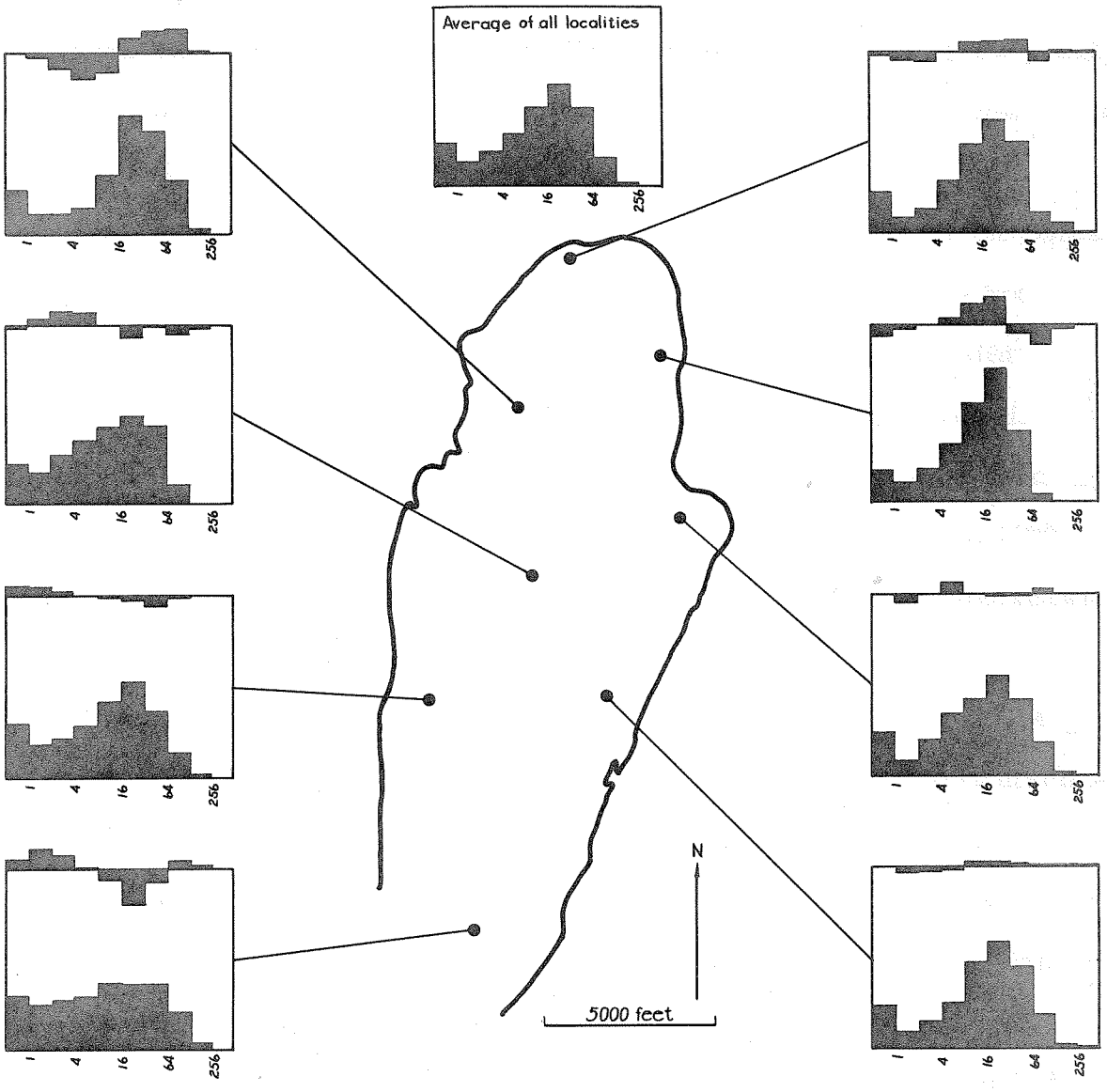

FIGURE 6

SIZE DISTRIBUTION OF CLASTS IN THE BLACKHAWK BRECCIA

Lower histogram shows distribution at each locality. Upper histogram shows deviation from average distribution. Class intervals are < 1, 1-2, 2-4, 4-8, 8-16, 16-32, 32-64, 64-128, 128-256, > 256 mm. Frequencies determined by measurements at 225 points on weathered surfaces in each locality.

tion zones generally contain many more varieties of marble than the homogeneous zones they separate. This three-dimensional jigsaw puzzle effect is the most distinctive lithologic characteristic by which Blackhawk-type breccias might be recognized in the geologic column.

Gold- and silver-bearing red hematite-stained gouge from the Santa Fe fault has been mined in numerous workings in the Member 4 breccia, which are without exception located near the distal edge of the slide, suggesting that the lower part of the overthrust block of Furnace limestone, as it fell from Blackhawk Mountain, became the forward portion of the resultant rockslide. Statistical study of the color of about 1500 clasts failed, however, to verify a similar correlation in the Blackhawk slide.

The limestone breccia along the distal end and western lateral edge of the Blackhawk slide is underlain by a persistent, but probably discontinuous, prism of "breccia" composed of disaggregated Old Woman sandstone (Figure 7) which was transported more than 4 miles northward by the slide. The contact between the limestone and sandstone breccias is usually marked by up to 6 inches of clayey green gouge, and is quite sharp, though occasionally scattered clasts of limestone are admixed with the sandstone "breccia" within one or two feet of the contact. Sandstone "breccia" is not exposed anywhere on the upper surface of the Blackhawk slide. Similarly, the sandstone "breccia" in the Member 4 breccia crops out only along the distal edge of the slide.

Clasts of quartzite breccia from Member 2 have been found in three widely separated places on the Blackhawk slide (Figure 8), though at present Member 2 quartzite breccia crops out only in a small area 1000 feet southeast of Surprise Spring. The blocks of quartzite breccia near

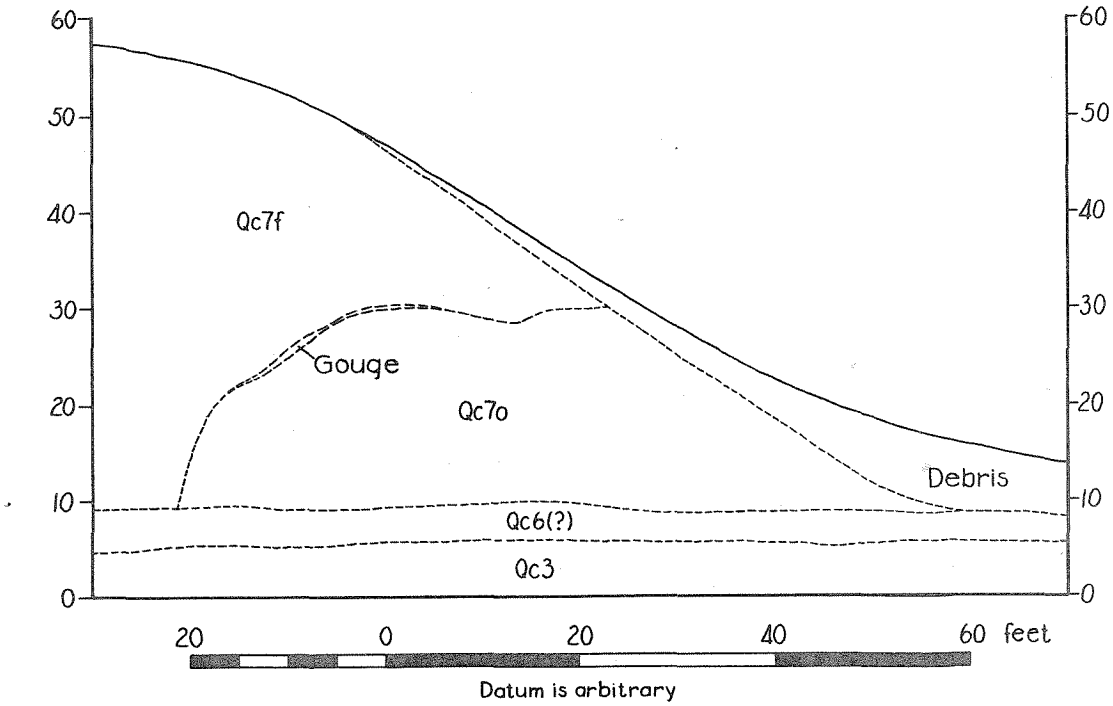

FIGURE 7

SANDSTONE "BRECCIA" IN THE BLACKHAWK SLIDE

Cross-section showing typical occurrence of sandstone "breccia" in the Blackhawk slide.

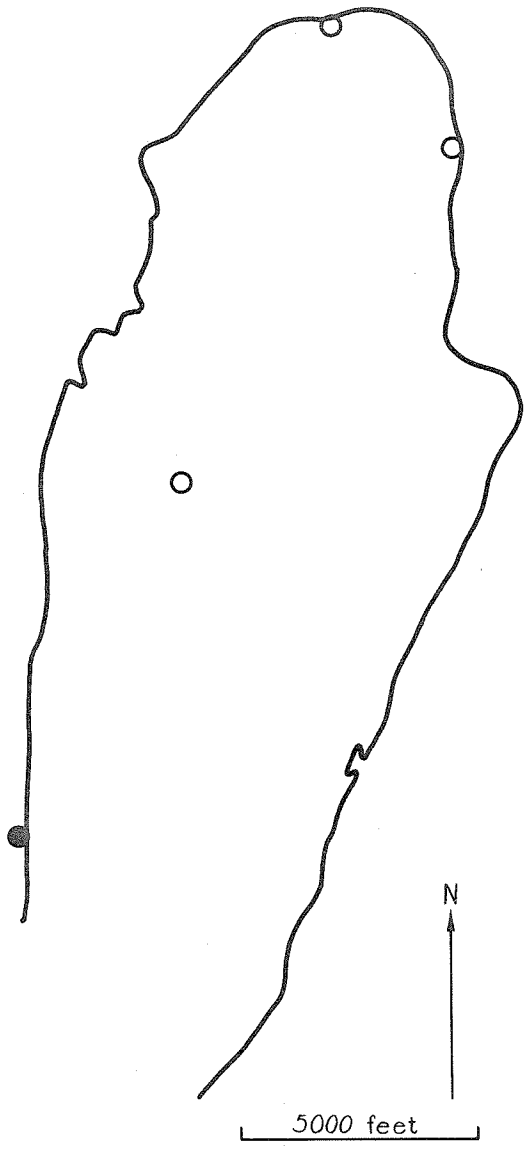

FIGURE 8

CLASTS OF QUARTZITE BRECCIA IN THE BLACKHAWK SLIDE

Open circles indicate localities where clasts of quartzite breccia occur. Solid circle shows sole location within Blackhawk area where quartzite breccia is exposed.

the center of the slide originated above the Santa Fe mine on Blackhawk Mountain; thus, the source of the quartzite clasts in the Member 2 breccia was near the present summit of Blackhawk Mountain.

Transport and deposition- The geological evidence implies that the Blackhawk slide was neither internally lubricated nor slow-moving, like a mudflow, but was a nearly nondeforming sheet of breccia which descended the gently inclined alluvial slope at a speed of more than 50 miles per hour. Similar evidence leads to the same conclusion about the Member 4 slide.

Simple mechanical considerations show that the velocity of the material in a moving mudflow increases monotonically from zero at the bed to a maximum at the free upper surface; therefore, the surficial material travels faster than the leading edge, eventually overtakes it, and is finally rolled under the advancing mudflow. This means that material at the forward edge of a mudflow was transported on the upper surface. In particular, if the Blackhawk slide were a mudflow, the sandstone "breccia" deposits at its distal edge should be accompanied, barring a remarkable coincidence, by similar deposits on its upper surface. Such deposits, however, are totally absent; therefore, the Blackhawk breccia descended the alluvial slope as a nearly nondeforming sheet sliding on a relatively thin, easily sheared lubricating layer.

If the fluid composing this lubricating layer exerted enough drag to prevent the breccia sheet from sliding faster than about 50 miles per hour, then it necessarily had a viscosity at least 10^4 times that of water. This is about the viscosity of unusually sticky mud. No trace of a mud layer exists anywhere along the contact of the Blackhawk breccia with the underlying Member 6 fanglomerate exposed near the mouth of Blackhawk Canyon.

Moreover, neither the marble breccia of which the slide is composed nor the cobble fanglomerate on which it rests readily forms mud when mixed with water. Hence, it is unlikely that the lubricating fluid was highly viscous mud; therefore, the speed of the slide was probably in excess of 50 miles per hour.

There are no mechanical reasons why the lubricating fluid could not have been water (or watery mud); however, the accumulation on the surface of the alluvial apron and on the slopes of Hill 3747 of the more than 10^7 cubic feet of water required is highly improbable. Thus, neither water nor mud are very likely as the fluids which lubricated the Blackhawk slide.

Air-lubrication hypothesis- Compressed air, rather than water or mud, probably was the lubricating fluid that supported the Blackhawk breccia sheet as it traversed the gently inclined alluvial apron. According to this idea, herein termed the "air-lubrication hypothesis," the breccia was launched at a speed of more than 100 miles per hour from a topographic step about 200 feet high (the "launching step") at the head of the alluvial slope; and, as it dropped, it trapped a cushion of compressed air on which it then rode down the alluvial slope, much as the slipper in a thrust-bearing moves along on a cushion of oil with no metal-to-metal contact (Figure 9).

The air-lubrication hypothesis explains all of the important physical features of the Blackhawk slide without ad hoc assumptions. (a) The high speed and nondeforming nature of the moving sheet of breccia resulted from the fact that the air layer, having low density and viscosity, was easily sheared. (b) The lateral ridges formed because leakage at the

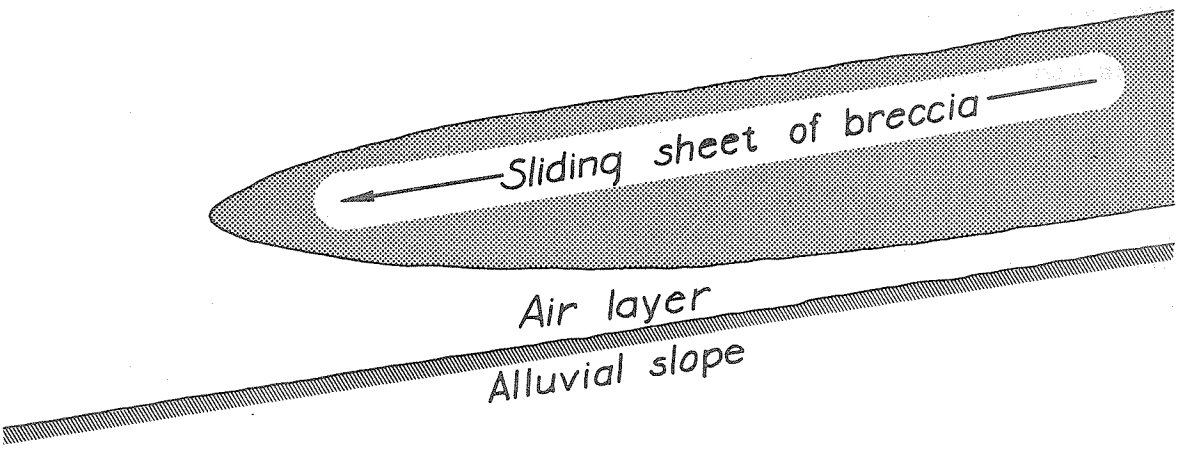

FIGURE 9

AIR-LUBRICATION HYPOTHESIS

sides of the slide allowed the lateral edges of the breccia sheet to fall and stop, forming walls which greatly slowed further leakage (Figure 10, which shows successive configurations in a fixed transverse cross-section). The zone of shearing is nowhere well-exposed; hence, no direct evidence for this explanation of the origin of the lateral ridges was found. (c) Leakage at the leading edge of the slide was much slower than at the sides because of the speed of the breccia; nevertheless, it did occur. Finally, the advancing front of the slide touched the ground and stopped abruptly. At first it was overrun by breccia from behind, forming the low rim and steep scarplike distal edge. (d) Then the zone of stopping travelled like a wave back up the length of the slide. The transverse ridges on the slide surface reflect successive positions of this zone. (e) The three-dimensional jigsaw puzzle effect resulted from the pervasive fracturing of large blocks by the impact. The fragments were not dispersed because no further motion ensued. (f) The breccia which overtopped the Hill 3747 ridge did not have sufficient forward velocity to be relaunched on the distal side of the crest; hence, it came to rest prematurely, stopping the breccia behind it, and causing the formation of new lateral ridges on the western and southwestern slopes of the hill.

The air-lubrication hypothesis thus explains qualitatively the principal features of the Blackhawk slide; but it is founded on the assumptions that a sufficiently high pressure gradient could be developed at the leading edge of the slide, and that adequate clearance could be maintained beneath it. These assumptions can only be justified by theoretical investigation of the mechanics of air-lubrication.

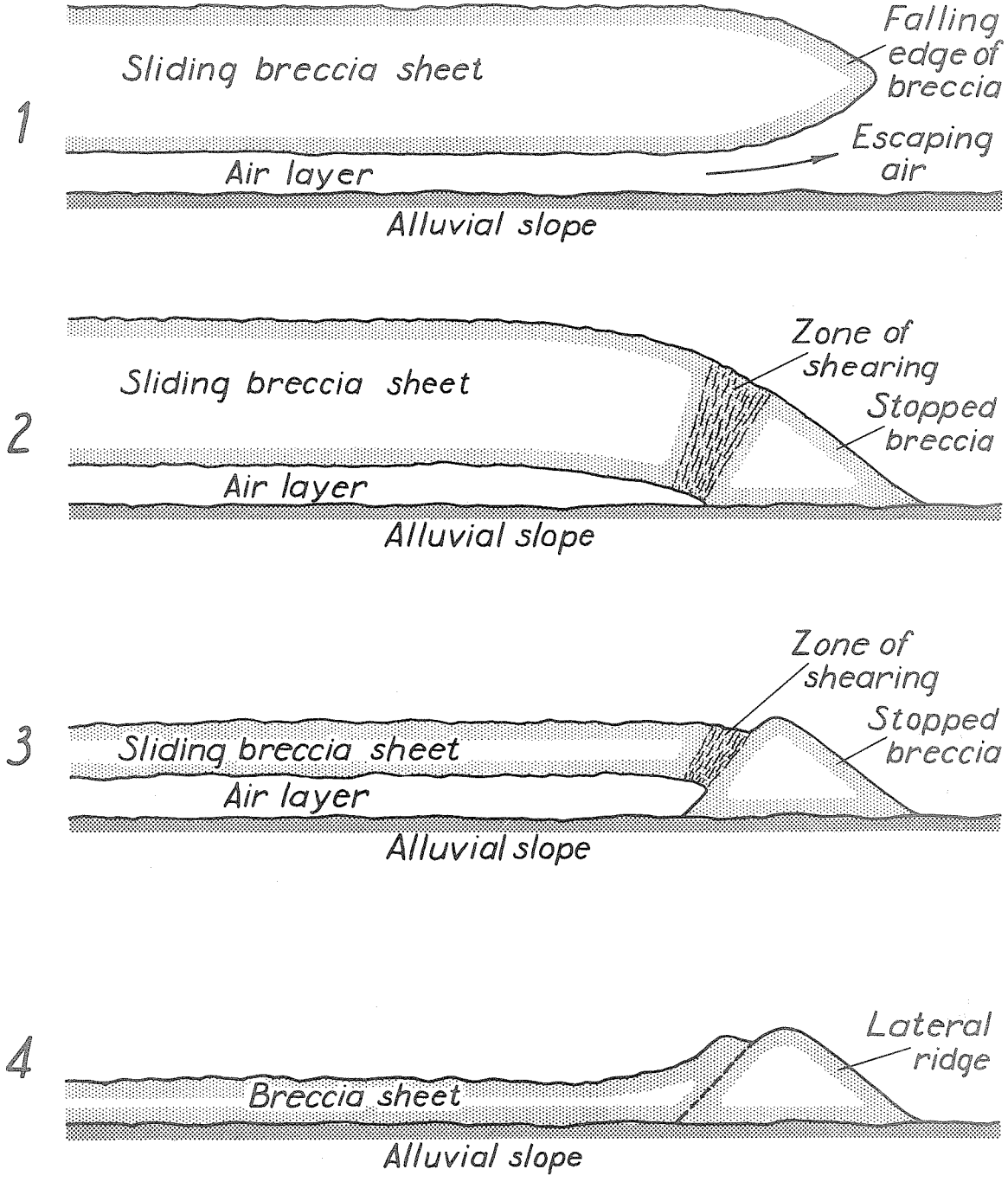

FIGURE 10

FORMATION OF LATERAL RIDGES

Air-lubrication theory

The primary problem in investigating the mechanics of air-lubrication of the Blackhawk slide is development of a theory of flow in the lubricating air layer. We will solve this problem as follows: (a) we start with the fundamental equations of fluid mechanics and perform the usual averaging process to separate the terms due to turbulent fluctuations; (b) we drastically simplify the equations by neglecting small terms; (c) we then obtain, by integration of the simplified continuity equation, a partial differential equation from which we can compute the thickness of the air layer provided we can find the velocity profile at each cross-section; and, finally, (d) we calculate the required velocity profiles by numerical integration of the simplified momentum equation.

Co-ordinate system and boundary conditions- We assume for simplicity that the breccia sheet slides with slowly varying velocity U_s over a horizontal plane immovable bed between frictionless parallel vertical walls. We choose a Cartesian co-ordinate system with its origin located in the plane of the bed at the foot of the launching step, with its positive x-axis directed horizontally parallel to U_s, and with its positive y-axis directed vertically upward perpendicular to the bed.

We wish to find the thickness of the air layer $h = h(x, t)$ and the drag on the breccia sheet $\tau_s = \tau(x, h, t)$ in terms of the atmospheric density and pressure ρ_a and p_a, the pressure at the base of the breccia sheet $p_s = p(x, h, t)$, the horizontal speed of the breccia sheet $U_s = U(x, h, t)$, the initial thickness of the air layer $h_i = h(x, t_o)$, and the thickness of

the air layer $h_o = h(x_o, t)$ at $x = x_o$ (defined below). The pressure p_s is given by

$$p_s = p_a + \rho_b b(g + \frac{\partial^2 h}{\partial t^2}), \tag{1a}$$

where ρ_b and $b = b(x, t)$ are the density and thickness of the breccia sheet, respectively. We shall assume

$$\frac{\partial^2 h}{\partial t^2} \ll g, \tag{1b}$$

so that we can treat p_s as a known function. We define $x = x_o$ as the least value of x for which our solution is valid; in practice x_o is determined by the condition (1b). The height h_o is fixed by the condition that the net mass flux near the step $Q_o = Q(x_o, t)$ is very nearly zero; hence, we take

$$Q_o = 0. \tag{1c}$$

Finally, the usual conditions on the normal and tangential velocities at the boundaries must be satisfied; hence,

$$U(x, 0, t) = 0, \quad V(x, 0, t) = 0, \tag{1d}$$

and

$$U(x, h, t) = U_s, \quad V(x, h, t) = \frac{\partial h}{\partial t}. \tag{1e}$$

Fundamental equations- The fundamental equations of fluid mechanics are (a) the continuity equation,

$$\frac{\partial \rho}{\partial t} + \nabla \cdot (\rho \underline{u}) = 0, \tag{2a}$$

(b) the momentum equation,

$$\rho \frac{\partial \underline{u}}{\partial t} + \rho(\underline{u} \cdot \nabla)\underline{u} = \rho \underline{X} - \nabla p - \mu \nabla \times (\nabla \times \underline{u}) + \frac{4}{3}\mu \nabla(\nabla \cdot \underline{u}), \tag{2b}$$

(c) the energy equation, which for an ideal gas is

$$\rho c_v \frac{\partial \theta}{\partial t} + \rho c_v (\underline{u} \cdot \nabla)\theta = -p(\nabla \cdot \underline{u}) + \Phi + \nabla \cdot (K \nabla \theta), \tag{2c}$$

in which the dissipation function Φ is given by

$$\Phi = \mu \{(\nabla \times \underline{u})^2 + 2\nabla \cdot [(\underline{u} \cdot \nabla)\underline{u}]\},$$

and (d) the equation of state of the fluid, which for an ideal gas is

$$p = \rho\theta(c_p - c_v). \tag{2d}$$

The viscosity of the fluid is implicitly assumed in these equations to be constant.

We separate the velocity in turbulent flow into two components, a slowly varying part called the "mean velocity," or simply the "velocity," and defined by

$$\underline{U} = \frac{1}{T} \int_t^{t+T} \underline{u} \, dt, \tag{3a}$$

in which T is long compared to the period of the turbulent fluctuations but short compared to the time of changes in the large scale flow regime, and a fluctuating part called the "fluctuation velocity" and defined by

$$\underset{\sim}{u} = \underline{u} - \underline{U}. \tag{3b}$$

A similar separation can be made for other fluctuating quantities. Substituting (3b) into (2), neglecting fluctuations in pressure and density,

assuming zero body force, averaging as in (3a) (Schlichting, 1955, p. 371), and denoting the resultant running average of a quantity by placing a bar over it, we obtain

$$\frac{\partial \rho}{\partial t} + \nabla \cdot (\rho \underline{U}) = 0, \tag{4a}$$

$$\rho \frac{\partial \underline{U}}{\partial t} + \rho(\underline{U} \cdot \nabla)\underline{U} = -\nabla p - \mu \nabla \times (\nabla \times \underline{U}) + \frac{4}{3}\mu \nabla(\nabla \cdot \underline{U}) - \overline{\rho(\tilde{\underline{u}} \cdot \nabla)\tilde{\underline{u}}}, \tag{4b}$$

$$\rho c_v \frac{\partial \theta}{\partial t} + \rho c_v (\underline{U} \cdot \nabla)\theta = -p(\nabla \cdot \underline{U}) + \overline{\Phi} + \nabla \cdot (K \nabla \theta), \tag{4c}$$

in which

$$\overline{\Phi} = \mu \{(\nabla \times \underline{U})^2 + 2\nabla \cdot [(\underline{U} \cdot \nabla)\underline{U}]\} + \mu \overline{\{(\nabla \times \tilde{\underline{u}})^2 + 2\nabla \cdot [(\tilde{\underline{u}} \cdot \nabla)\tilde{\underline{u}}]\}},$$

and finally

$$p = \rho \theta (c_p - c_v). \tag{4d}$$

These equations for the mean velocity in turbulent flow are exactly the same as the corresponding equations for the velocity in non-turbulent flow except that the momentum and energy equations contain additional terms, the "Reynolds stress" term and the "turbulent dissipation" term, respectively.

Simplification of equations- We neglect the temperature rise due to viscous dissipation with respect to that due to compression, and disregard the transfer of heat by thermal conduction; that is, we take

$$\overline{\Phi} = 0, \tag{5a}$$

and

$$\nabla \cdot (K \nabla \theta) = 0. \tag{5b}$$

Inserting (5) in (4c), eliminating θ by means of (4d), and using (4a), we obtain

$$\frac{\partial}{\partial t} \ln (p/\rho^{\gamma}) + (\underline{U} \cdot \nabla) \ln (p/\rho^{\gamma}) = 0, \tag{6a}$$

in which $\gamma = c_p/c_v$; hence, under the assumptions (5) the entropy of the fluid does not vary along the streamlines. Observing that the fluid is initially isentropic, and using (6a), we find

$$\left(\frac{p}{p_a}\right)^m = \frac{\rho}{\rho_a}, \tag{6b}$$

where $m = 1/\gamma = c_v/c_p$. Thus, under the assumptions (5), the energy equation (4c) and the equation of state (4d) reduce to the adiabatic law (6b).

Expanding (4a) and (4b), assuming two-dimensional flow, subtracting (4a) from (2a), and substituting the result in the last term in (4b), we obtain

$$\left[\frac{\partial h}{\partial x}\right] \quad \left[\frac{V}{U_s}\right] \quad \left[\frac{h}{p}\frac{\partial p}{\partial x}\right] \quad \left[\frac{V}{U_s}\frac{h}{p}\frac{\partial p}{\partial y}\right] \left[\frac{h}{U_s}\frac{1}{p}\frac{\partial p}{\partial t}\right]$$

$$\frac{\partial U}{\partial x} + \frac{\partial V}{\partial y} + \frac{U}{\rho}\frac{\partial \rho}{\partial x} + \frac{V}{\rho}\frac{\partial \rho}{\partial y} + \frac{1}{\rho}\frac{\partial \rho}{\partial t} = 0, \tag{7a}$$

$$\left[\frac{V}{U_s}\right] \quad \left[\frac{\partial h}{\partial x}\right] \quad \left[\frac{V}{U_s}\right] \quad \left[\frac{1}{R}\frac{V}{U_s}\frac{\partial h}{\partial x}\right] \quad \left[\frac{1}{R}\left(\frac{\partial h}{\partial x}\right)^2\right] \quad \left[\frac{1}{R}\right]$$

$$\rho\frac{\partial U}{\partial t} + \rho U\frac{\partial U}{\partial x} + \rho V\frac{\partial U}{\partial y} = -\frac{\partial p}{\partial x} + \frac{1}{3}\mu\frac{\partial^2 V}{\partial x\partial y} + \frac{4}{3}\mu\frac{\partial^2 U}{\partial x^2} + \mu\frac{\partial^2 U}{\partial y^2}$$

$$\left[\frac{\partial h}{\partial x}\right] \quad \left[1\right] \quad \left[\frac{h}{p}\frac{\partial p}{\partial x}\right] \quad \left[\frac{h}{p}\frac{\partial p}{\partial y}\right]$$

$$-\rho\left\{\frac{\partial\overline{\tilde{u}^2}}{\partial x} + \frac{\partial\overline{\tilde{u}\tilde{v}}}{\partial y} + \frac{\overline{\tilde{u}^2}}{\rho}\frac{\partial\rho}{\partial x} + \frac{\overline{\tilde{u}\tilde{v}}}{\rho}\frac{\partial\rho}{\partial y}\right\}, \qquad (7b)$$

$$\left[\frac{h}{U_s^2}\frac{\partial^2 h}{\partial t^2}\right] \left[\frac{V}{U_s}\frac{\partial h}{\partial x}\right] \quad \left[\frac{V^2}{U_s^2}\right] \quad \left[\frac{1}{R}\frac{\partial h}{\partial x}\right] \quad \left[\frac{1}{R}\frac{V}{U_s}\left(\frac{\partial h}{\partial x}\right)^2\right]\left[\frac{1}{R}\frac{V}{U_s}\right]$$

$$\rho\frac{\partial V}{\partial t} + \rho U\frac{\partial V}{\partial x} + \rho V\frac{\partial V}{\partial y} = -\frac{\partial p}{\partial y} + \frac{1}{3}\mu\frac{\partial^2 U}{\partial x\partial y} + \mu\frac{\partial^2 V}{\partial x^2} + \frac{4}{3}\mu\frac{\partial^2 V}{\partial y^2}$$

$$\left[\frac{\partial h}{\partial x}\right] \quad \left[1\right] \quad \left[\frac{h}{p}\frac{\partial p}{\partial x}\right] \quad \left[\frac{h}{p}\frac{\partial p}{\partial y}\right]$$

$$-\rho\left\{\frac{\partial\overline{\tilde{u}\tilde{v}}}{\partial x} + \frac{\partial\overline{\tilde{v}^2}}{\partial y} + \frac{\overline{\tilde{u}\tilde{v}}}{\rho}\frac{\partial\rho}{\partial x} + \frac{\overline{\tilde{v}^2}}{\rho}\frac{\partial\rho}{\partial y}\right\}, \qquad (7c)$$

and

$$\left(\frac{p}{p_a}\right)^m = \frac{\rho}{\rho_a}. \qquad (7d)$$

The quantities in square brackets indicate the relative order of magnitude of the respective terms above which they are placed (after multiplication by h/U_s in (7a), and by $h/\rho U_s^2$ in (7b) and (7c)). They are calculated by noting that

$$\left[U\right] = \left[U_s\right],$$

$$\left[\frac{\partial}{\partial x}\right] = \left[\frac{\partial h}{\partial x}\ \frac{\partial}{\partial h}\right],$$

$$\left[\frac{\partial}{\partial y}\right] = \left[\frac{1}{h}\right],$$

$$\left[\frac{\partial U}{\partial h}\right] = \left[\frac{U_s}{h}\right],$$

and

$$\left[\frac{\partial V}{\partial h}\right] = \left[\frac{V}{h}\right],$$

in which "[x]" means "order of magnitude of x."

We make the assumptions, to be verified a posteriori, (a) that the thickness of the air layer changes slowly,

$$\frac{\partial h}{\partial x} \ll 1, \tag{8a}$$

$$\frac{\partial h}{\partial t} \ll U_s, \tag{8b}$$

and, therefore, because V is the same order of magnitude as $\partial h/\partial t$, the vertical component of velocity is small,

$$\frac{V}{U_s} \ll 1, \tag{8c}$$

(b) that the vertical acceleration of the slide is small enough that

$$\frac{\partial^2 h}{\partial t^2} \ll \frac{U_s^2}{h}, \tag{8d}$$

(c) that the Reynolds number is very large,

$$R = \frac{\rho U_s h}{\mu} \gg 1, \tag{8e}$$

(d) that the boundaries are so rough that

$$R\lambda = \frac{\rho U_s h}{\mu} \lambda \gg 1, \tag{8f}$$

where λh is about one-tenth of the boundary relief, and (e) that the pressure is large enough that

$$\frac{h}{p} \frac{\partial p}{\partial x} \ll 1, \tag{8g}$$

and

$$\frac{h}{p} \frac{\partial p}{\partial y} \ll 1, \tag{8h}$$

Neglecting small terms in (7), in accordance with (8), we obtain

$$\frac{\partial U}{\partial x} + \frac{\partial V}{\partial y} + \frac{U}{\rho} \frac{\partial \rho}{\partial x} + \frac{1}{\rho} \frac{\partial \rho}{\partial t} = 0, \tag{9a}$$

$$\frac{\partial p}{\partial x} = - \rho \frac{\partial \overline{\tilde{u}\tilde{v}}}{\partial y}, \tag{9b}$$

$$\frac{\partial p}{\partial y} = - \rho \frac{\partial \overline{\tilde{v}^2}}{\partial y}, \tag{9c}$$

and

$$\left(\frac{p}{p_a}\right)^m = \frac{\rho}{\rho_a}. \tag{9d}$$

Substituting (9d) into (9c), integrating with respect to y, and using the condition that the fluctuation velocity is small at the boundaries, we obtain

$$\left(\frac{p}{p_s}\right)^{1-m} = 1 - (1 - m) \frac{\rho_s \overline{\tilde{v}^2}}{p_s} \tag{10}$$

from which, because the second term on the righthand side is small, we

find

$$p = p_s; \tag{11}$$

hence, we obtain

$$\frac{\partial U}{\partial x} + \frac{\partial V}{\partial y} + \frac{U}{\rho_s}\frac{\partial \rho_s}{\partial x} + \frac{1}{\rho_s}\frac{\partial \rho_s}{\partial t} = 0 \tag{12a}$$

in place of (9a), and

$$\frac{\partial \overline{\tilde{u}\tilde{v}}}{\partial y} = -\frac{1}{\rho_s}\frac{\partial p_s}{\partial x} \tag{12b}$$

in place of (9b). The $\overline{\tilde{u}^2}$ and $\overline{\tilde{v}^2}$ components of the Reynolds stress, therefore, do not appreciably affect the flow. Equations (12a) and (12b) together form the simplified set of differential equations on which the analysis of flow in the lubricating air layer is based.

Formal solution- Integrating (12a) with respect to y from 0 to h, and using (1), we obtain

$$\int_0^h \frac{\partial U}{\partial x}\,dy = -\frac{\partial h}{\partial t} - \frac{1}{\rho_s}\frac{\partial \rho_s}{\partial x}\int_0^h U\,dy - \frac{h}{\rho_s}\frac{\partial \rho_s}{\partial t}; \tag{13}$$

but, again using (1), we observe that

$$\frac{\partial}{\partial x}\int_0^h U\,dy = U_s\frac{\partial h}{\partial x} + \int_0^h \frac{\partial U}{\partial x}\,dy; \tag{14}$$

hence, combining (13) and (14), and letting $\alpha = (y/h)$, we obtain a partial differential equation,

$$\frac{1}{U_s}\frac{\partial h}{\partial t} = \frac{\partial h}{\partial x} - \frac{1}{\rho_s U_s}\frac{\partial}{\partial x}\left\{\rho_s U_s h\int_0^1 \frac{U}{U_s}\,d\alpha\right\} - \frac{h}{\rho_s U_s}\frac{\partial \rho_s}{\partial t}, \tag{15}$$

from which we can compute h provided we can find U/U_s as a function of α. The quantity in curly brackets is the net mass flux at (x, t).

According to Prandtl's "mixing-length" theory of turbulent flow

(Schlichting, 1955, pp. 383-389), which gives surprisingly accurate results for the type of flow considered here despite the fact that it is not a strictly correct representation of the turbulence, the Reynolds shear stress is related to the mean velocity by

$$-\rho\,\overline{\tilde{u}\tilde{v}} = \rho\ell^2\left(\frac{\partial U}{\partial y}\right)^2 \operatorname{sgn}\left(\frac{\partial U}{\partial y}\right), \tag{16}$$

where ℓ is the "mixing-length." Because it is impossible to find ℓ a priori, we guess its form. This is more straightforward than it sounds, because we know (a) that ℓ is a relatively smooth function of position that is independent of the fluid velocity, (b) that, as $y \to 0$, $\ell \to \kappa(\lambda h + y)$, and, as $y \to h$, $\ell \to \kappa(\lambda h + h - y)$, and (c) that accuracy in our choice for ℓ is mainly important only near the boundaries, where the velocity gradient is high. The simplest function fitting these requirements is

$$\ell = \frac{\kappa}{h}(\lambda h^2 + hy - y^2) = \kappa h(\lambda + a - a^2), \tag{17}$$

where $a = (y/h)$. Both the proportionality constant κ and the additive constant λ are empirically determined; for most types of boundary roughness κ is approximately 0.4 and λh is about one-tenth of the boundary relief.

Substituting (16) and (17) into (12b), integrating with respect to y, letting $(hA(x)/\rho_s)\partial p_s/\partial x$ be the integration constant, and rearranging, we find

$$\frac{\partial U}{\partial a} = U_s\left|\frac{h}{\kappa^2\rho_s U_s^2}\frac{\partial p_s}{\partial x}\right|^{1/2}\frac{|a-A|^{1/2}}{\lambda + a - a^2}\operatorname{sgn}\left\{(a-A)\frac{\partial p_s}{\partial x}\right\}, \tag{18}$$

in which $\alpha = (y/h)$. Integrating (18) with respect to α, and using (6b) and the condition (1d) that $U = 0$ on $\alpha = 0$, we obtain

$$\frac{U}{U_s} = B^{1/2} \int_0^{\alpha} \frac{|\beta - A|^{1/2}}{\lambda + \beta - \beta^2} \operatorname{sgn}(\beta - A)\, d\beta, \tag{19a}$$

in which we define

$$B^{1/2} = \left| \frac{h}{\kappa^2 \rho_a U_s^2} \left(\frac{p_a}{p_s}\right)^m \frac{\partial p_s}{\partial x} \right|^{1/2} \operatorname{sgn}\left(\frac{\partial p_s}{\partial x}\right), \tag{19b}$$

and

$$B = \frac{h}{\kappa^2 \rho_a U_s^2} \left(\frac{p_a}{p_s}\right)^m \frac{\partial p_s}{\partial x}. \tag{19c}$$

From the condition (1e) that $U = U_s$ on $\alpha = 1$ we find

$$B^{-1/2} = \int_0^1 \frac{|\beta - A|^{1/2}}{\lambda + \beta - \beta^2} \operatorname{sgn}(\beta - A)\, d\beta, \tag{20}$$

from which A can be computed as a function of B.

When $\partial p_s/\partial x \to 0$, corresponding to $A \to \infty$, we find, noting that $\lambda \ll 1$,

$$\frac{\partial U}{\partial \alpha} \to - \frac{U_s}{2 \ln \lambda (\lambda + \alpha - \alpha^2)}, \tag{21a}$$

$$\frac{U}{U_s} \to - \frac{1}{2 \ln \lambda} \ln \left[\frac{(\lambda + \alpha)(1 + \lambda)}{\lambda(1 + \lambda - \alpha)} \right], \tag{21b}$$

and

$$\int_0^1 \frac{U}{U_s}\, d\alpha \to \frac{1}{2}. \tag{21c}$$

Substituting (19) into (15), multiplying both sides by U_s, letting $U_o = U(x_o, h, t)$, defining

$$F = \frac{U_s}{U_o}\left(\frac{p_s}{p_o}\right)^m , \tag{22a}$$

$$G = B^{1/2}\int_0^1\int_0^\alpha \frac{|\beta - A|^{1/2}}{\lambda + \beta - \beta^2}\ \mathrm{sgn}\,(\beta - A)\, d\beta\, d\alpha, \tag{22b}$$

and

$$H = \frac{\partial h}{\partial x} - \frac{1}{F}\frac{\partial}{\partial x}(FGh) - \frac{h}{\rho_s U_s}\frac{\partial \rho_s}{\partial t} \tag{22c}$$

and using (6b), we obtain

$$\frac{\partial h}{\partial t} = U_s H, \tag{22d}$$

from which we can compute h by step-by-step numerical integration. The quantity $Q = \rho_a U_o FGh$ is, from (15), the net mass flux at (x, t).

Letting $\tau_s = \tau(x, h, t)$ be the shear stress, or drag, on the breccia sheet, defining the drag function

$$S = \frac{\tau_s}{\rho_a U_s^2}\left(\frac{p_a}{p_s}\right)^m , \tag{23a}$$

combining (16), (17), and (18), and using (6b), we obtain

$$S = \kappa^2 B(1 - A). \tag{23b}$$

When $\partial p_s/\partial x \to 0$, we find from (16), (17), and (21a)

$$S \to -\frac{\kappa^2}{4(\ln \lambda)^2} . \tag{24}$$

We can integrate (22d) numerically by (a) computing $H_o = H(x, t_o)$ from (22c) and the known functions ρ_a, p_a, p_s, U_s, h_i, and h_o (performing the indicated differentiations numerically), (b) substituting H_o into (22d) to get $\partial h/\partial t = (\partial h/\partial t)_o$ at time $t = t_o$, then (c) multiplying $(\partial h/\partial t)_o$ by an increment of time $\Delta_1 t$ to obtain the corresponding change in h, from which $h_1 = h(x, t_o + \Delta_1 t) = h_o + \Delta_1 h$ and hence $H_1 = H(x, t_o + \Delta_1 t)$ can be determined, so that the process can be repeated step-by-step.

In order to compute G from (22b) we first numerically integrate (20) to find the values of B corresponding to a suitably chosen set of values of A and λ (Table 3); then numerically carrying out the second integration, and substituting the result into (22b), we obtain for each of the previously determined values of B the corresponding values of G (Table 3). Using the previously determined values of A, B, and λ, we also compute the drag function S from (23b) (Table 3).

Equations (19c), (20), (22), and (23) together comprise the general solution of the problem of flow in the lubricating air layer.

TABLE 3

VALUES OF B, G, AND S FOR SELECTED VALUES OF A AND λ

	λ = 0.001			λ = 0.010		
A	B	G	S	B	G	S
0.500	- ∞	∞	- ∞	- ∞	∞	- ∞
0.510	-41.088	25.691	-3.221	-73.051	19.000	-5.727
0.550	- 2.164	6.272	-0.156	- 4.268	4.963	-0.307
0.580	- 0.874	4.157	-0.0587	- 1.740	3.337	-0.117
0.600	- 0.540	3.364	-0.0346	- 1.059	2.702	-0.0678
0.620	- 0.362	2.835	-0.0220	- 0.706	2.329	-0.0429
0.650	- 0.236	2.368	-0.0132	- 0.465	1.940	-0.0260
0.700	- 0.132	1.876	-0.00634	- 0.257	1.546	-0.0123
0.800	- 0.0552	1.344	-0.00177	- 0.109	1.135	-0.00349
0.855	---	---	---	- 0.0784	1.000	-0.00182
0.900	- 0.0282	1.047	-0.00045	- 0.0571	0.907	-0.00091
0.922	- 0.0246	1.000	-0.00031	---	---	---
0.950	- 0.0204	0.927	-0.00016	- 0.0416	0.810	-0.00033
1.000	- 0.0132	0.772	0.00000	- 0.0296	0.710	0.00000
1.100	- 0.0092	0.683	0.00015	- 0.0216	0.647	0.00035
1.200	- 0.0074	0.647	0.00024	- 0.0177	0.620	0.00057
2.000	- 0.0032	0.562	0.00051	- 0.0077	0.551	0.00123
∞	0.0000	0.500	0.00084	0.0000	0.500	0.00188
-1.000	0.0032	0.438	0.00101	0.0077	0.449	0.00245
-0.200	0.0074	0.353	0.00143	0.0177	0.380	0.00340
-0.100	0.0092	0.317	0.00161	0.0216	0.351	0.00380
0.000	0.0132	0.224	0.00211	0.0296	0.290	0.00474
0.050	0.0204	0.075	0.00310	0.0416	0.190	0.00632
0.078	0.0246	0.000	0.00363	---	---	---
0.100	0.0282	-0.049	0.00406	0.0571	0.092	0.00822
0.145	---	---	---	0.0784	0.000	0.0107
0.200	0.0552	-0.344	0.00707	0.109	-0.136	0.0140
0.300	0.132	-0.875	0.0148	0.257	-0.547	0.0288
0.350	0.236	-1.368	0.0245	0.465	-0.940	0.0484
0.380	0.362	-1.835	0.0359	0.706	-1.330	0.0700
0.400	0.540	-2.364	0.0518	1.059	-1.702	0.102
0.420	0.874	-3.157	0.0811	1.740	-2.337	0.161
0.450	2.164	-5.272	0.190	4.268	-3.963	0.376
0.490	41.088	-24.691	3.353	73.051	-18.000	5.961
0.500	∞	- ∞	∞	∞	- ∞	∞

Blackhawk slide

The air-lubrication hypothesis is based on the assumptions that a sufficient pressure gradient was developed at the leading edge of the Blackhawk slide, and that adequate clearance was maintained beneath it. We have developed the theory of flow in the lubricating air layer as a means of justifying these assumptions on theoretical grounds. We proceed by: (a) estimating the numerical values of ρ_a, p_a, p_s, U_s, h_i, and h_o for the Blackhawk slide; then (b) verifying the validity of the approximations and assumptions of the theory for this set of numerical values; and finally (c) making a preliminary computation from which we conclude that the air-lubrication hypothesis probably provides the correct explanation of the mode of transport and deposition of the Blackhawk slide.

Initial and boundary conditions- The theory of air-lubrication is not applicable unless (among other restrictions) $\partial h/\partial t \ll U_s$, $\partial h/\partial x \ll 1$, $\partial^2 h/\partial t^2 \ll g$; therefore, we cannot choose the initial clearance h_i arbitrarily. For this reason, we proceed by trial and error to find the function h_i for which $\partial h/\partial t$ is as small as possible; in practice, the h_i thus obtained satisfies the second and third restrictions as well. We then calculate the motion backward in time from this initial configuration to the earliest configuration for which the theory is valid. This method assumes that the breccia rapidly settles to an equilibrium height above the alluvial surface after launching, and it implicitly ignores the likely possibility that at first the breccia oscillates vertically with substantial amplitude.

We next calculate the motion forward in time until the thickness of

the air layer at some point becomes less than an arbitrarily chosen amount (about 0.1 ft). In general, this happens at a point near the front of the sliding breccia sheet. The object of the calculation is to determine how far the breccia travels before this initial impact occurs.

The clearance h_o at $x = x_o$ is fixed by the condition (1c) that $Q_o = 0$; but, regardless of the magnitude of h_o, Q_o cannot be zero unless $\partial p_s/\partial x > 0$. The pressure at $x = x_o$, therefore, at first drops until the thickest part of the breccia sheet has passed. This means that, for an air-lubricated slide to travel a long distance, its thickest part must be well forward, as it is in the Blackhawk slide; otherwise the proximal end impacts before the distal end. On the other hand, if the maximum thickness is too far forward, the pressure gradient at the front is so high that the leading edge settles quickly.

At the launching step the breccia was necessarily travelling less than 400 ft sec^{-1}, the speed it would have acquired if it had dropped without friction from the summit of Blackhawk Mountain to the head of the alluvial slope. On the other hand, it had to be moving fast enough to become airborne in the vicinity of the Mill fault, where the gradient of the former surface changed abruptly from nearly level to about 25 percent (Plate 1). The requisite velocity was at least 200 ft sec^{-1} (135 mi hr^{-1}).

We assume that the drag on the breccia sheet was negligible, that is, that

$$\tau_s \ll \rho_b \, bg \sin \psi, \tag{25}$$

where $\psi = \tan^{-1} 0.06$ is the angle of inclination of the alluvial slope. In accordance with (25),

$$U_s^2 = U_o^2 + 2g(x - x_o) \sin \psi. \tag{26}$$

Taking U_o to be 200 ft sec^{-1} and the length of the slide to be 24×10^3 ft, we find that the breccia traversed the alluvial slope in 85 sec, and reached a maximum velocity of 365 ft sec^{-1} (250 mi hr^{-1}).

Because the initial impact occurred at the leading edge of the slide, causing the zone of stopping to travel back up the breccia sheet, the thickness of the Blackhawk slide lobe as now observed is greater than the thickness it had while in motion. Assuming that the thickness was approximately doubled in the stopping process, we conclude that at the moment of impact the thickness of the breccia sheet increased uniformly from 30 ft at $x = x_o$ to a maximum of 50 ft approximately 4000 ft from the leading edge, then decreased smoothly to zero from the maximum point to the leading edge. The thickness at any time prior to the impact can be found from the fact that, at a given point fixed in the breccia, the product of the thickness and the velocity is a constant.

We calculate the pressure p_s from the thickness b by means of the equation

$$p_s = p_a + \rho_b b g, \tag{27}$$

where $\rho_b = 2.5$ gm cm^{-3} and $p_a = 1$ atm (corresponding to $p_a = 1.2 \times 10^{-3}$ gm cm^{-3}).

Verification of assumptions- Condition (1e) that $V(x, h, t) = \partial h/\partial t$ implicitly assumes that leakage up through the sliding breccia was negligible. If, however, leakage was not negligible, (1e) would be written

$$V(x, h, t) = \frac{\partial h}{\partial t} + q, \tag{28}$$

where q is the volume flux of air up through the breccia. We wish to show that q actually is negligible.

In the one-dimensional case Darcy's law is

$$q = - \frac{k}{\mu} \frac{\partial p}{\partial y}, \tag{29a}$$

where k is the permeability of the breccia; the equation of continuity for steady one-dimensional flow is

$$\frac{\partial}{\partial y}(\rho q) = 0; \tag{29b}$$

and the equation of state for isentropic flow of an ideal gas originating in the lubricating air layer is

$$\left(\frac{p}{p_a}\right)^m = \frac{\rho}{\rho_a}. \tag{29c}$$

Combining these equations, and using the fact that the viscosity of an ideal gas is proportional to the square root of its absolute temperature, we find

$$\frac{\partial^2 p^{1/n}}{\partial y^2} = 0, \tag{30}$$

where $n = 2/(3m + 1)$. Solving for p, we obtain

$$p = \{ p_s^{1/n} - \frac{y - h}{b} (p_s^{1/n} - p_a^{1/n} \}^n. \tag{31}$$

Substituting (31) into (29a), and letting μ_s be the viscosity of the air at the lower surface of the breccia sheet, we obtain

$$q = \frac{kn}{\mu_s b} p_s \{1 - (p_a/p_s)^{1/n}\}. \tag{32}$$

Taking $n = 0.64$, $\mu_s = 0.025$ centipoise, $b = 100$ feet, $p_s = 8.5$ atm, and $q < 0.1$ cm sec^{-1} (0.2 ft min^{-1}), we find $k < 1.5$ darcy. Inasmuch as we expect a material like the Blackhawk breccia to have a permeability of

about 1 darcy (Muskat, 1946, p. 113), we conclude that condition (1e) is satisfied.

The pressure gradient due to leakage required to support the breccia must be at least $-\rho_b g$ at the base of the breccia; but, by differentiation of (31), we find

$$\left.\frac{\partial p}{\partial y}\right|_{y=h} = -\rho_b g n \{1 - (p_a/\rho_b b g)^{1/n}\}, \tag{33}$$

which is less than the required gradient. At the upper surface of the slide the gradient due to leakage is too large. Therefore, either the permeability or the density of the breccia (or both) was about 20 percent smaller at the bottom of the breccia sheet than at the top. This small difference cannot be observed in the field.

To verify the conditions (8) we note that $[U_s] = 200$ ft sec^{-1}, $[h] = 1$ ft, $[\rho] = 10^{-3}$ gm cm^{-3}, $[\mu] = 10^{-4}$ cgs, $[\lambda] = 10^{-2}$, $[p] = 1$ atm, and $[\partial p/\partial x] = 10^{-2}$ atm ft^{-1}. Substituting in (8d), we find that

$$\frac{\partial^2 h}{\partial t^2} \ll 4 \times 10^4 \text{ ft sec}^{-2}, \tag{34a}$$

which is not as restrictive as the condition (1b) that $\partial^2 h/\partial t^2 \ll g$; substituting in (8e), we find that

$$[R] = 2 \times 10^6 \gg 1, \tag{34b}$$

in (8f), that

$$[R\lambda] = 2 \times 10^4 \gg 1, \tag{34c}$$

and in (8g), that

$$\left[\frac{h}{p}\frac{\partial p}{\partial x}\right] = 10^{-2} \ll 1. \tag{34d}$$

Because $\partial p/\partial y \ll 1$ according to (11), we find for (8h),

$$\left[\frac{h}{p}\frac{\partial p}{\partial y}\right] \ll 1. \tag{34e}$$

We verify assumptions (8a), (8b), and (8c) during the computation of h.

The assumption (25) that $\tau_s \ll \rho_b bg \sin\psi$ is, using (23a), equivalent to

$$S \ll \left(\frac{p_a}{p_s}\right)^m \frac{\rho_b bg}{\rho_a U_s^2} \sin\psi \tag{35a}$$

or, inserting numerical values,

$$S \ll 1 \tag{35b}$$

for U_s greater than 10 ft. In the case of the Blackhawk slide, S is never greater than about 0.1; therefore, we conclude that the drag on the breccia sheet was in fact negligible.

Computations and conclusions- Preliminary computations show that to calculate the complete motion of the Blackhawk slide using a desk calculator would require at least 400 hours; therefore, it was impossible to carry out the complete calculation for this thesis. However, the preliminary work does indicate that the thickness of the air layer decreased from about 1 foot immediately after launching to approximately 0.1 foot at the moment of impact; thus, it is highly probable that the air-lubrication hypothesis is correct and, therefore, that the Blackhawk breccia traversed the alluvial slope on a lubricating layer of compressed air.

REFERENCES CITED

De Groot, Henry (1890) San Bernardino County - Mines and mining: Calif. State Mining Bureau, 10th Annual Report of State Mineralogist. pp. 520-533

Dibblee, T. W., Jr. (1958) Tertiary stratigraphic units of western Mojave Desert, California: A. A. P. G. Bull. v. 42 pp. 135-144

Guillou, R. B. (1953) Geology of the Johnston Grade area, San Bernardino County, California: Calif. State Div. Mines Special Report 31 pp. 1-18

Heim, Albert (1882) Der Bergsturz von Elm: Zeits. deutschen geol Gesellsch. v. 34 pp. 74-115

Hershey, O. H. (1902) Some Tertiary formations of southern California: Am. Geol. v. 29 pp. 349-372

Hewett, D. F., and J. J. Glass (1953) Two uranium-bearing pegmatite bodies in San Bernardino County, California: Am. Mineralogist. v. 38 pp. 1040-1050

Muskat, Morris (1946) The flow of homogeneous fluids through porous media: 763 pp. Edwards, Ann Arbor, Michigan.

Richmond, J. F. (1954) Petrology and structure of the San Bernardino Mountains north of Big Bear Lake: PhD thesis, Stanford University, Stanford, California, 145 pp.

Schlichting, Hermann (1955) Boundary layer theory: 535 pp. McGraw-Hill, New York

Vaughan, F. W. (1922) Geology of San Bernardino Mountains north of San Gorgonio Pass: Calif. Univ. Pub. Geol. Sci. v. 13 pp. 319-411

Wilmarth, M. G. (1938) Lexicon of geologic names of the United States: U. S. G. S. Bull. 896 2396 pp.

Woodford, A. O., and T. F. Harriss (1928) Geology of Blackhawk Canyon, San Bernardino Mountains, California: Calif. Univ. Pub. Geol. Sci. v. 17 pp. 265-304